CORSICA OPHIOLITES: GEOCHEMISTRY AND PETROGENESIS OF BASALTIC AND METABASALTIC ROCKS

Emilio Saccani*[✉], Gianfranco Principi**, Francesca Garfagnoli** and Francesco Menna**

* Dipartimento di Scienze della Terra, Università di Ferrara, Italy.
** Dipartimento di Scienze della Terra, Università di Firenze, Italy.
[✉] *Corresponding author, e-mail: sac@unife.it*

Keywords: *Ophiolite, geochemistry, petrogenesis, Piedmont-Ligurian Ocean, Alpine Corsica.*

ABSTRACT

This paper presents a systematic geochemical characterization of the basaltic and metabasaltic rocks from the Alpine Corsica ophiolites. The various ophiolitic units of Alpine Corsica can basically be subdivided into two main types: (1) high-pressure/low-temperature, metamorphic ophiolites belonging to the Lower Schistes Lustrés (LSL) and Upper Schistes Lustrés (USL) Complexes and (2) the non-metamorphic, upper ophiolitic units.

Basaltic and metabasaltic rocks from all these units display many common geochemical characteristics, which indicate a common genesis in a mid-ocean ridge setting. However, on the bases of their high field strength element (HFSE) and rare earth element (REE) distribution, two main geochemical types can be recognized. One type has normal MORB-type (N-MORB) geochemical features, being characterized by flat N-MORB normalized HFSE patterns, slight depletion in Th, U, Ta and variable depletion of light REE (LREE) with respect to medium REE (MREE). This type is volumetrically prevalent and is found in metabasalts from the LSL and USL, as well as in basalts from the upper ophiolitic units. The other type has transitional MORB-type (T-MORB) geochemical features, as it shows slightly enriched N-MORB normalized HFSE patterns, slight enrichment in Th, U, Ta and LREE enrichment with respect to MREE. This type is observed in metabasaltic rocks from the Santo Pietro di Tenda Unit (USL) and in basalts from the Nebbio and from the bottom of the Balagne units.

A distinguishing geochemical feature of basaltic and metabasaltic rocks from the Alpine Corsica ophiolites is a marked heavy REE (HREE) fractionation with respect to MREE. The $(Sm/Yb)_N$ ratios range from 1.1 to 2.6, but in most cases are > 1.5. This feature is interpreted as a garnet signature, which can be related to the melting of a heterogeneous mantle source characterized by garnet-bearing mafic/ultramafic layers. Semi-quantitative modelling of the REE data for the N-MORBs indicates that these rocks may have derived from small-degree (< 8%) partial melting of a depleted MORB-type peridotitic source bearing small volumes of garnet-pyroxenite relics. The differential degree of partial melting of this source can explain the significant range of variation of LREE/MREE ratios, as well as the high $(Sm/Yb)_N$ ratios observed in the studied N-MORB rocks. In addition, the N-MORB rocks most likely derived from compositionally similar mantle sources and much of the internal chemical variation in these rocks is more likely due to differential partial melting rather than different enrichments of their mantle sources. Semi-quantitative modelling of the REE data for the T-MORBs indicates that these rocks may have been derived from small-degree (< 5%) partial melting of a lithospheric mantle source bearing garnet-pyroxenite relics. They could represent products extruded in the ocean-continent transition zone during the initial stage of oceanic opening, whereas N-MORBs may represent volcanic sequences formed in more internal paleo-oceanic positions after the onset of the oceanic spreading.

INTRODUCTION

The Alpine Corsica occupies the northeastern portion of the Corsica Island (Fig. 1a) and is composed of a complex pile of mostly east-vergent tectonic units of the Alpine orogenesis (l.s.). Ophiolite massifs of Alpine Corsica, together with those of the Western Alps and Northern Apennines, represent remnants of the Piedmont-Ligurian oceanic basin, a branch of the Mesozoic Tethys, which formed between the divergent European and Adria passive margins.

Alpine Corsica basically includes two types of ophiolitic units, showing contrasting styles of deformation and metamorphism (see Malavieille et al., 1998 for a complete description), which were emplaced and juxtaposed onto the European continental margin in consequence of the convergence between the European and Adria plates during the Late Cretaceous - Early Tertiary times. Most of the studies on Alpine Corsica ophiolites are devoted to their syn-orogenic tectonic evolution (e.g., Principi and Treves, 1984; Durand-Delga, 1984; Warburton, 1986; Durand-Delga et al., 1997; Lahondère and Guerrot, 1997; Malavieille et al., 1998; Marroni and Pandolfi, 2003; Principi et al., 2004; Bortolotti and Principi, 2005). On the other hand, the geochemical characterization and the petrogenesis of most of the Alpine Corsica ophiolitic units are still lacking. Only the Rio Magno (Padoa et al., 2001, 2002), Pineto and Nebbio

(Saccani et al., 2000) Units were studied in detail. Very few data on the Balagne Unit (Venturelli et al., 1979; Durand-Delga et al., 1997), Inzecca Unit (Beccaluva et al., 1977; Venturelli et al., 1981), and the Cap Corse region (Venturelli et al., 1981) are available. By contrast, no geochemical data are available for most of the Schistes Lustrés units, though these are the volumetrically most abundant ophiolites in Corsica.

A systematic geochemical characterization of the Alpine Corsica ophiolites may give effective informations on the composition and characteristics of the oceanic crust that was forming the Piedmont-Ligurian Ocean, which may provide, in turn, useful constraints for further studies on the entire pre-orogenic and syn-orogenic evolution of the Alpine Corsica portion of the orogenic belt. Therefore, the present work aims to provide such geochemical constraints, by presenting the geochemical and petrogenetic characteristics of volcanic and metavolcanic rocks of the oceanic crust preserved in the different ophiolitic units of Alpine Corsica. In addition, these data are used to establish the genetic relationships between the different ophiolitic units. This paper is intended as a first step of a comprehensive work that will be completed by the authors with an impending article on the geological significance and geodynamic evolution of the Alpine Corsica ophiolites in the general framework of the Corsica-Alps-Apennine system.
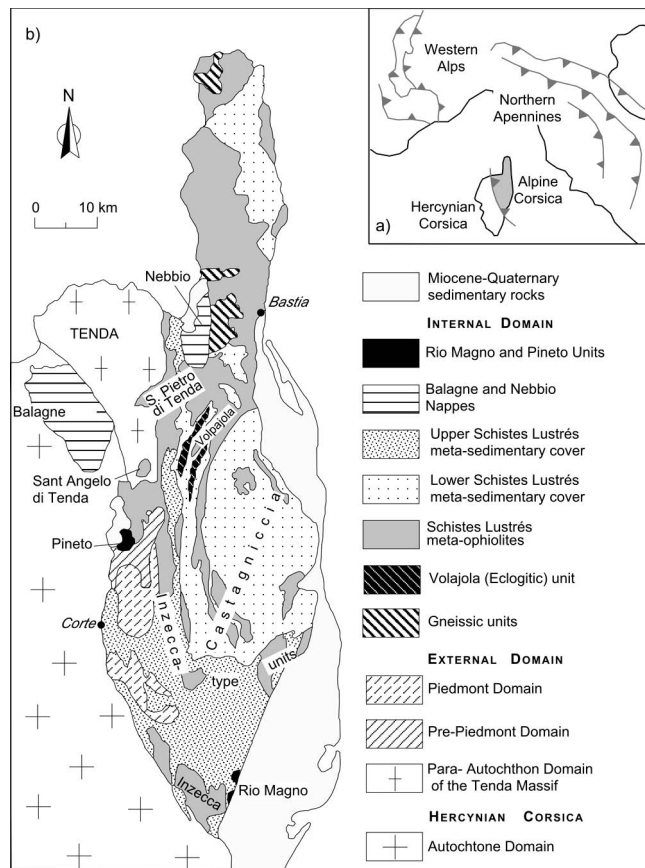
Fig. 1 - a) Location of the Alpine Corsica with respect to the Hercynian Corsica and Western Alps and Northern Apennine orogenic belts; b) simplified geological map of the Alpine Corsica (modified after Lahondère, 1996).

GENERAL GEOLOGICAL SETTING

The Corsica Island can be subdivided into two distinct geological domains: the Hercynian Corsica and the Alpine Corsica (Fig. 1a). The Alpine Corsica is composed by a complex pile of mostly east-vergent tectonic units of the Alpine orogenesis (l.s.) derived from both oceanic and continental domains (e.g., Durand-Delga, 1984).

According to previous authors (e.g., Durand-Delga, 1984; Durand-Delga et al., 1997), the Alpine Corsica can be subdivided into two portions (Fig. 1b): (1) an Internal Domain, mainly represented by units of the Piedmont-Ligurian Ocean; and (2) an External Domain formed by continental/sub-continental units of the European Plate paleo-margin (para-autochthonous units).

Starting from the middle Cretaceous, the Piedmont-Ligurian oceanic basin underwent a convergence and was involved in a subduction process, associated with the development of high pressure/low temperature (HP/LT) metamorphism, followed by large-scale extension, which lead to the collapse of the orogenic wedge. This convergence also resulted in the emplacement of ophiolitic units showing very low-grade ocean-floor metamorphism, such as, the Balagne, Nebbio, Pineto and Rio Magno Units (Fig. 1b).

The Upper Cretaceous HP/LT metamorphic phase is recorded by the deformation and metamorphism observed in both oceanic and continental rocks belonging to the Schistes Lustrés Complex (Maluski, 1977; Lahondère and Guerrot, 1997). Afterwards, partial re-equilibration in the greenschist facies of the HP-LT units syn-kinematically occurred together with E-SE verging deformations during syn-orogenic exhumation (e.g., Warburton, 1986; Brunet et al., 2000). The Schistes Lustrés Complex overlies the tectonic units of the External Domain, some of which were also largely involved in the HP/LT subduction phase (e.g., Gibbons et al., 1986; Brunet et al., 2000).

At the top of the Schistes Lustrés, an assemblage of units characterized by very low-grade ocean-floor metamorphism is recognized. They are represented by ophiolitic units (Balagne, Nebbio, Pineto, and Rio Magno Units) consisting of Jurassic ophiolite sequences and related Upper Jurassic - Upper Cretaceous sedimentary covers (e.g., Durand-Delga, 1978; Saccani et al., 2000; Padoa et al., 2001; Rossi et al., 2002; Marroni and Pandolfi, 2003).

MAIN GEOLOGICAL FEATURES OF THE STUDIED OPHIOLITIC UNITS OF THE ALPINE CORSICA

The Schistes Lustrés Complex

Durand-Delga (1984) subdivided the Schistes Lustrés Complex into two main groups: (1) the Upper Schistes Lustrés (USL), showing comparatively lower metamorphic grade mainly under lawsonite-bearing blueschist-facies conditions. They include the Inzecca, Santo Pietro di Tenda, Sant'Angelo di Tenda Units and other Inzecca-type ophiolitic units (Caron et al., 1979); and (2) the Lower Schistes Lustrés (LSL) showing comparatively higher metamorphic imprint, up to glaucophane-bearing eclogite conditions (Ohnenstetter et al., 1976; Gibbons et al., 1986; Lahondère, 1996). They are represented by the Castagniccia Unit (Caron et al., 1979).

The Sant'Angelo di Tenda Unit (USL) represents a tectonic klippe of Schistes Lustrés on the top of the metagranitoids of the Tenda Massif (Fig. 1b). It is composed mainly by metabasalts and pillow metabreccias with laminated lenses of serpentinites at the basal tectonic contact.

The Inzecca Unit (USL) shows low-grade HP/LT facies and typically consists (from bottom to top) of: metaserpentinites, ophicalcites, ophiolitic sandstones, pillow basalts, metacherts, alternating schists and metacarbonates, schists and quartzites, quartzites with levels of arenaceous metacarbonates and metapelites (Erbajolo Formation). Locally, (e.g., Punta di Corbara), there are sub-units with successions consisting of: metaserpentinites, metophicalcites locally followed by lenses of ophiolitic metabreccias and metasandstones, then metacherts and metapelites (Erbajolo Fm.). These successions range in age from Middle-Late Jurassic (U/Pb age of zircons in plagiogranites of the Inzecca area: 161±1 Ma: Ohnenstetter et al., 1981) to Cretaceous (Durand-Delga, 1978; 1984).

The Santo Pietro di Tenda Unit (USL) is formed by low-grade metaophiolites very similar to those of the Inzecca Unit. This succession is considered Late Jurassic - Cretaceous in age based on the strong similarity with the Inzecca Unit.

The Castagniccia Unit (LSL) represents an ophiolitic complex showing very composite tectonic and stratigraphic features. For simplicity, two types of ophiolitic units: the Castagniccia Unit *s.s.* and the Volpajola Unit are described. The Castagniccia Unit *s.s.* consists of metaophiolitic masses showing ambiguous stratigraphic contacts with their cover successions. The Volpajola Unit (LSL) is an eclogitic unit largely characterized by retrograde metamorphism under

blueschist and greenschist facies. It is composed by a peripheral serpentinitic shell including deformed aggregates of metaophiolites associated with metacherty-limestones and lenses of gneisses.

The Balagne nappe

This unit occupies the westernmost (external) position, to the west of the metagranitoids of the Tenda Massif (Fig. 1b). The Balagne nappe is formed by a pile of tectonic units (Nardi et al., 1978; Durand-Delga, 1984), where the westernmost units are superposed on the Hercynian crystalline basement and its Tertiary sedimentary cover (para-autochthonous).

According to Nardi et al. (1978) the Balagne Unit consists (from bottom to top) of: (1) Cenomanian-Campanian calcareous flysch (Marino et al., 1995). (2) Middle Eocene sandstone (Marino et al., 1995). (3) an ophiolitic succession, with serpentinite, gabbro, pillow basalts, and associated sedimentary covers (Marroni and Pandolfi, 2003). (4) Turbiditic units (Marino et al., 1995). According to De Wever and Danelian (1995), the age of the Balagne ophiolites is middle Callovian - Kimmeridgian, whereas radiometric ages (U/Pb SHRIMP on zircons) of trondhjemitic dykes intruded in gabbros yielded an age of 169±3 Ma (Rossi et al., 2002). A transitional-type mid-ocean ridge basalt (T-MORB) composition of the basaltic rocks has been recognized by many authors (Venturelli et al., 1979; Durand-Delga et al., 1997; Saccani et al., 2000). The Balagne ophiolites have previously been interpreted as an oceanic crust developed during the early phase of oceanic spreading (Sagri et al., 1982; Durand-Delga, 1984; Gardin et al., 1994; Durand-Delga et al., 1997; Marroni and Pandolfi, 2003; Principi et al., 2004).

The Nebbio Unit

This unit is a small non-metamorphic thrust-sheet, which lies over the metamorphic terrains of the Schistes Lustrés (Fig. 1b). Two groups of units can be distinguished: (1) The lower unit, which is composed of a continental basement (pre-Hercynian metamorphic rocks) and its sedimentary cover; (2) The upper unit, which is characterized by an ophiolitic succession similar to that of the Balagne (Saccani et al., 2000) starting from T-MORB pillow basalts followed by radiolarites and massive limestones, correlative of the radiolarites and the Calpionella-limestones of the Balagne Nappe.

The Pineto Unit

This unit (Fig. 1b) is mainly represented by an intrusive, stratified sequence composed by troctolites, pegmatoid gabbros, Fe-gabbros and minor dunites, locally intruded by doleritic dykes (Durand-Delga, 1978; Saccani et al., 2000). The intrusive suite is covered by a thin and discontinuous basaltic level followed by a sedimentary succession starting with cherts and then pelites with late Berriasian "palombini"-like limestones, marls with thin quartzites levels and the Albian-Cenomanian, calcareous flysch (Rossi et al., 1994).

The Rio Magno Unit

This unit discontinuously crops out at the southeastern border of Alpine Corsica (Fig. 1b). It is tectonically superposed on the Schistes Lustrés of the Inzecca Unit and consists of: pillow and massive basalts with normal MORB (N-MORB) geochemical affinity (Padoa et al., 2001) overlain by a middle Berriasian-Valanginian sedimentary cover, which is correlative of the Palombini Shales of Northern Apennines (Padoa and Durand-Delga, 2001).

PETROGRAPHY

Sampling was focused on volcanic and subvolcanic rocks in units affected only by ocean-floor metamorphism, namely the Balagne, Nebbio, Rio Magno, and Pineto Units, as well as on metavolcanic rocks in units displaying HP/LT metamorphic imprint, that is, the Castagniccia and Volpajola Units for the LSL, along with the Sant'Angelo di Tenda, Inzecca, Santo Pietro di Tenda, and some Inzecca-type units for the USL. A summary of the petrographic characteristics of these rocks is given in Table 1.

Basaltic rocks from the Balagne, Nebbio, Rio Magno, and Pineto Units include a variety of lithological facies (Table 1) and are extensively affected by low-grade ocean-floor hydrothermal metamorphism, which resulted in recrystallization of the primary igneous phases, while the primary igneous textures are preserved. The main mineralogical substitutions are illustrated in Table 1. Variable amounts of amygdales and/or veins, usually filled with calcite and epidote, are observed in many samples. These rocks display a wide range of textural varieties, from aphyric to porphyric and glomeroporphyric (Table 1). Phenocrysts are represented by plagioclase and rarely by olivine. Groundmass is commonly ophitic and sub-ophitic; nonetheless the Balagne basalts have hyalophitic groundmass displaying chlorite replacements.

Metabasaltic rocks from the Lower and Upper Schistes Lustrés Units collectively contain mineral assemblages of several metamorphic facies, and it is common for individual samples to contain two or three texturally distinct assemblages or mineral relics of different facies.

Eclogites can be subdivided into two textural and mineralogical varieties (Table 1). The most common eclogites display nematoblastic texture with a mineralogical assemblage, which testify for a metamorphic overprinting in the glaucophane-lawsonite facies (Table 1).

Blueschists generally consist of garnet porphyroblasts set in a fine-grained, nematoblastic matrix (Table 1). Retrograde mineralogical assemblages are locally observed (Table 1). Magmatic relics are rarely observed; they mainly consist of plagioclase porphyroblasts, which are partially recrystallized into albite + epidote.

The greenschist facies metabasites have a mineral assemblage (Table 1) indicating that they represent retrograde rocks originated from the blueschists. These rocks are fine- to medium-grained and show a well-developed schistosity. However, non-foliated varieties subordinately occur. The metabasites from the Sant'Angelo di Tenda Unit are very fine-grained and display a weak (volumetrically predominant) to moderate (subordinate) crenulation cleavage defined by chlorite. Textural relics of primary igneous phases can be observed in samples exhibiting weak crenulation cleavage. They consist of porphyroblasts of plagioclase (up to 3 mm in size) completely transformed into albite + epidote and, subordinately of small porphyroblasts of clinopyroxene relatively fresh.

Table 1 - Summary of the main petrographic characteristics of mafic volcanic and metavolcanic rocks from Corsica ophiolites.

Volcanic and subvolcanic rocks:

rock type	unit	sampled facies	rock texture	phenocryst assemblage	groundmass texture	groundmass assemblage	alteration minerals
basalt	Balagne	pillow, M.L.F.	porphyric (PI<10) glomeroporphyric (PI ~ 40)	pl (ol)	hyalophitic	pl, glass	ab, cc, chl
basalt	Nebbio	pillow M.L.F.	porphyric/aphiric porphyric (PI<10)	pl pl	ophitic sub-ophitic	pl, cpx (Fe- Ti-ox) pl, cpx (Fe- Ti-ox)	prh, cc, ep, chl prh, cc, ep, chl
basalt	Rio Magno	pillow, M.L.F.	aphiric	-	ophitic/sub-ophitic	pl, cpx	prh, chl
basalt	Pineto	dyke, pillow, breccia	porphyric (PI<10)	pl (ol)	ophitic/sub-ophitic	pl, cpx	prh, chl, ser, tr

High-pressure/low-temperature metamorphic volcanic and subvolcanic rocks:

rock type	unit	rock texture	mineral assemblage	porphyroblast assemblage	retrograde assemblage	post-kinematic assemblage	magmatic relics
eclogite	Vopajola	porphyroblastic nematoblastic	grt+omp gln+lws+grt+omp+qz (±rt±ap±ttn)	grt -	- gln+lws±bar±chl±ep	- bar±prh±ep	- -
blueschist	LSL (USL)	nematoblastic	gln+lws+ep+qz (±rt±ap±ttn) [1]	grt	bar±chl±act±ab± ep±phe	bar±phe	(pl)
metabasite	USL (LSL)	foliated (non-foliated) crenulated[2]	ab+chl+ep+act/tr+qz ab+chl+ep+qz	- -	- -	- -	- (pl+cpx)

Abbreviations, M.L.F.: massive lava flow; PI: porphyric index; pl: plagioclase; ol: olivine; cpx: clinopyroxene; ab: albite; cc: calcite; chl: chlorite; ox: oxide; ep: epidote; prh: prhenite; ser: sericite; tr: tremolite; grt: garnet; omp: omphacite; gln: glaucophane; lws: lawsonite; qz: quartz; rt: rutile; ap: apatite; ttn: titanite; bar: barroisite; act: actinolite; phe: phengite. ( ): rare occurrence. (1) observed in Fe-rich metabasites (meta-ferrobasalts); (2) texture occurring only in the Sant'Angelo di Tenda Unit.

ANALYTICAL METHODS

The geochemical discussion presented in this paper is based on a total of about 170 samples of basaltic and metabasaltic rocks. Geochemical data (and relative analytical techniques, accuracies and detection limits) on about 20 samples from the Rio Magno, Nebbio and Pineto Units have already been presented by Saccani et al. (2000) and Padoa et al. (2001). 150 new analyses on basalts from the Balagne and Pineto Units, as well as on HP/LT metabasaltic rocks from the Sant'Angelo di Tenda, LSL, USL, Inzecca, and Eclogitic units are presented herein. These rocks were analyzed for major and some trace elements (Zn, Ni, Co, Cr, V, Rb, Ba, Pb, Sr, Zr, Y), by X-ray fluorescence (XRF) on pressed-powder pellets. Calibration for XRF methods was done with international reference samples (some of which were also run as unknowns for the determination of accuracy and detection limits), and the matrix correction method proposed by Lachance and Trail (1966) was applied. Mean accuracies are generally less than 2% for major oxides, and 5% for trace element determinations, while the detection limits for trace elements are: Zn, Ba = 5 ppm; Ni, Co, Cr, V, Rb = 1 ppm; Sr, Zr, Y = 2 ppm. Volatile contents were determined as loss on ignition at 1000°C.

The trace elements Sc, Nb, Hf, Ta, Th, and U, and the rare earth elements (REE) were determined on about 50 samples by inductively coupled plasma-mass spectrometry (ICP-MS). The accuracy of the data and detection limits were evaluated using results for international standard rocks and the blind standards included in the sample set. Accuracy ranges from 2 to 7 relative percent, with the exception of Nb and Ta (12%), and U (9%). Detection limits (in ppm) are: Sc = 0.29; Nb, Hf, Ta = 0.02; Th, U = 0.01; La, Lu, Tm = 0.10; Ce, Ho = 0.20; Pr, Sm, Gd, Dy, Er, Yb = 0.02; Nd = 0.07; Eu, Tb = 0.01. All analyses were performed at the Department of Earth Science of Ferrara University using a ARL Advant-XP automated X-ray spectrometer and a VG Elemental Plasma Quad PQ2 Plus spectrometer. Results for representative samples are presented in Table 2. The whole data set of analyses can be obtained upon request from the corresponding author.

GEOCHEMISTRY

Alteration effects

All the basalt and metabasite samples show varying degrees of mineralogical transformation occurred during ocean-floor and/or HP/LT metamorphism and as such they can be expected to have suffered selective element mobility, especially involving the large ion lithophile elements

Table 2 - Bulk-rock major (wt%) and trace (ppm) element analyses for selected volcanic and metavolcanic rocks from Corsica ophiolites.

	Balagne				Nebbio				Rio Magno			
Locality	Colle San Colombano	Colle San Colombano	Navaccia Valley	Navaccia Valley	Oletta	Oletta	Saint Florent	Saint Florent	Poretta	Poretta	Saint Antoine	Saint Antoine
Sample	CO119B	CO120B	CO138B	CO139B	CO1N[1]	CO4N[1]	CO10N[1]	CO11N[1]	C20[2]	C23[2]	CORM2[2]	C37D[2]
Rock	Bas	Bas	Bas	Bas	Bas	Bas	Bas	Bas	Bas	Bas	Bas	B.And
Note	pillow	pillow	m.l.f.	pillow	m.l.f.	pillow	pillow	pillow	pillow	pillow	m.l.f.	m.l.f.
XRF analyses:												
SiO_2	49.75	46.30	45.59	52.07	49.87	52.29	49.10	49.09	45.06	47.73	46.15	55.02
TiO_2	2.07	1.60	1.60	1.63	2.12	2.10	1.87	2.33	1.99	1.17	1.48	1.15
Al_2O_3	18.24	15.89	12.35	14.76	15.81	16.52	16.88	17.25	15.31	18.94	16.89	14.47
Fe_2O_3	1.00	0.79	1.01	0.81	1.26	1.05	1.09	1.27	1.17	1.09	1.23	1.01
FeO	6.64	5.30	6.76	5.43	8.38	7.00	7.25	8.45	7.80	7.25	8.21	6.75
MnO	0.20	0.11	0.11	0.08	0.13	0.14	0.14	0.17	0.16	0.15	0.16	0.13
MgO	6.61	5.24	5.91	7.27	7.35	4.66	8.33	5.90	12.82	8.58	8.26	7.00
CaO	6.90	12.13	14.00	6.79	6.81	7.10	6.69	6.78	5.42	5.31	9.68	6.74
Na_2O	3.72	5.12	3.46	5.02	5.39	6.49	4.34	4.78	3.61	3.36	3.23	4.25
K_2O	2.37	0.31	0.57	0.86	0.13	0.05	0.83	0.41	0.05	2.51	0.03	0.04
P_2O_5	0.35	0.31	0.24	0.17	0.36	0.31	0.35	0.36	0.25	0.14	0.17	0.13
L.O.I.	2.15	6.91	8.37	5.22	2.40	2.29	3.13	3.23	6.36	3.77	4.50	3.29
Total	99.98	100.01	99.98	100.11	100.00	100.00	100.00	100.00	100.00	100.00	100.00	100.00
Mg#	63.9	63.8	60.9	70.5	61.0	54.2	67.2	55.4	74.5	67.8	64.2	64.9
Zn	81	69	76	80	87	65	80	128	100	74	96	69
Ni	112	48	47	163	66	100	82	32	80	131	83	85
Co	43	22	20	50	30	39	30	27	40	44	45	34
Cr	166	267	133	47	135	190	164	121	315	296	266	213
V	242	188	193	183	253	262	244	284	296	248	314	216
Rb	46	5	10	13	3	2	10	12	16	51	16	14
Ba	67	42	80	70	42	41	38	36	89	90	57	51
Pb	2	2	<d.l.	4	8	5	4	3	8	9	6	8
Sr	240	164	198	189	273	118	261	160	108	34	59	264
Zr	224	166	111	37	322	281	274	311	176	125	136	103
Y	41	32	30	29	47	46	42	48	48	32	39	29
ICP-MS analyses:												
Sc	26.9	29.4	22.8	27.1	27.3	29.7	35.2	29.7	41.4	33.0	38.9	30.3
La	7.64	5.36	5.02	3.40	9.14	7.24	7.98	10.20	4.37	3.60	4.42	4.53
Ce	22.4	14.5	15.4	11.7	26.3	19.25	21.5	28.6	14.2	12.6	13.9	14.2
Pr	3.72	2.44	2.59	2.07	4.25	3.06	3.42	4.71	2.60	2.21	2.46	2.60
Nd	18.0	12.1	14.3	11.9	21.7	16.3	18.1	23.1	14.7	11.8	13.4	15.0
Sm	5.11	3.48	4.45	4.00	6.36	5.34	5.73	6.44	4.97	3.84	4.41	5.02
Eu	1.62	1.25	1.29	1.16	1.95	1.92	1.94	2.23	1.55	1.23	1.38	1.78
Gd	5.61	3.98	5.46	4.81	6.97	7.09	7.40	7.29	5.51	4.20	4.79	5.22
Tb	1.03	0.69	0.88	0.81	1.24	1.27	1.26	1.36	1.01	0.76	0.85	0.79
Dy	6.29	4.13	5.49	5.12	7.49	8.43	8.51	8.04	6.77	4.98	5.68	4.69
Ho	1.36	0.88	1.08	1.00	1.49	1.77	1.70	1.58	1.52	1.13	1.26	0.95
Er	3.71	2.37	2.90	2.66	4.11	5.12	5.02	4.41	4.29	3.13	3.66	2.58
Tm	0.56	0.34	0.41	0.37	0.63	0.71	0.69	0.66	0.63	0.47	0.54	0.39
Yb	3.43	2.17	2.40	2.23	3.90	4.27	4.44	4.15	3.93	3.06	3.49	2.45
Lu	0.49	0.31	0.30	0.28	0.53	0.59	0.62	0.56	0.54	0.42	0.50	0.34
Nb	7.41	5.13	4.85	4.74	5.03	4.07	8.06	8.87	2.17	1.91	2.11	1.39
Hf	6.35	4.83	3.25	2.87	4.60	4.77	5.47	5.82	3.21	2.67	2.87	2.85
Ta	0.35	0.32	0.22	0.18	0.63	0.61	0.60	0.58	0.16	0.14	0.19	0.13
Th	0.29	0.30	0.37	0.45	0.45	0.43	0.48	0.52	0.15	0.16	0.13	0.12
U	0.13	0.13	0.15	0.18	0.14	0.22	0.16	0.18	0.05	0.05	0.04	0.05
Zr/Y	5.47	5.15	3.70	1.27	6.89	6.06	6.45	6.49	3.66	3.91	3.50	3.55
Nb/Y	0.18	0.16	0.16	0.16	0.11	0.09	0.19	0.19	0.05	0.06	0.05	0.05
$(La/Sm)_N$	0.97	0.99	0.73	0.55	0.93	0.88	0.90	1.02	0.57	0.60	0.65	0.58
$(Sm/Yb)_N$	1.66	1.78	2.06	1.99	1.81	1.39	1.43	1.72	1.41	1.39	1.41	2.28
$(La/Yb)_N$	1.60	1.77	1.50	1.09	1.68	1.22	1.29	1.76	0.80	0.84	0.91	1.33
$(Dy/Yb)_N$	1.23	1.27	1.53	1.54	1.29	1.32	1.28	1.30	1.15	1.09	1.09	1.28

Abbreviations, SPT: Santo Pietro di Tenda; Inz.-type: Inzecca-type; SAT: Sant'Angelo di Tenda; Castag.: Castagniccia; Bas: basalt; B.And: Basaltic andesite; Met-Bas: metabasalt; Met-B.And: metabasaltic andesite; Met-Fe-Bas: meta-ferrobasalt; Met-And: metaandesite; Bls: blueschist; m.l.f.: massive lava flow; n.d. = not determined; <d.l.: below detection limits. Fe_2O_3 = FeO X 0.15; Mg# = 100 X Mg/(Mg+Fe^{2+}), where Mg = MgO/40 and Fe = FeO/72. (1): data from Saccani et al. (2000); (2): data from Padoa et al. (2001).

Table 2 (*continued*)

	Pineto						Upper Schistes Lustrés						
Unit	Pineto						Inzecca Punta Corbara	Inzecca Punta Corbara	Inzecca Defilé	Inzecca Defilé	SPT	SPT	SPT
Locality	Pineto	Rio Casaluna	Rio Casaluna	Rio Casaluna	Ponte Leccia	Ponte Leccia					S. Pietro di Tenda	Biguglia	Pont de Lano
Sample	CO37P[1]	CO40P[1]	C48[1]	C49[1]	CO 88P	CO 89P	CO123PC	CO122PC	CO124I	CO125I	CO13	CO24	CO43
Rock	Bas	Bas	Bas	Bas	Bas	Bas	Met-Bas	Met-Fe-Bas	Met-Bas	Met-Bas	Met-Bas	Met-Bas	Met-Bas
Note	dyke	dyke	dyke	dyke	pillow	breccia	dyke	dyke	dyke	n.d.	pillow	n.d.	n.d.
XRF analyses:													
SiO_2	48.52	49.52	48.98	49.03	49.63	49.65	48.58	41.56	49.62	50.57	47.66	49.02	49.02
TiO_2	1.09	1.78	1.19	1.08	1.61	1.64	1.16	3.74	1.62	1.72	1.75	2.41	1.70
Al_2O_3	16.22	15.99	16.53	15.78	17.52	16.87	15.42	15.62	16.77	14.11	14.04	16.55	16.51
Fe_2O_3	0.96	1.13	1.01	0.85	0.96	0.96	1.10	2.17	1.36	1.27	1.26	1.40	1.17
FeO	6.41	7.53	6.73	5.67	6.42	6.38	7.35	14.45	9.05	8.46	8.39	9.33	7.82
MnO	0.11	0.11	0.13	0.08	0.18	0.16	0.18	0.21	0.20	0.15	0.14	0.15	0.16
MgO	10.84	8.68	9.32	11.31	8.91	8.14	10.11	6.94	6.34	9.66	10.84	7.62	7.46
CaO	10.71	8.45	10.25	9.86	5.90	6.39	6.14	7.04	5.76	6.28	8.29	5.03	7.40
Na_2O	3.04	4.32	3.54	3.31	4.76	5.21	3.13	3.67	3.12	4.89	2.93	3.82	5.17
K_2O	0.03	0.02	0.03	0.04	0.30	0.11	0.73	0.63	2.79	0.07	0.89	1.53	0.02
P_2O_5	0.38	0.33	0.40	0.39	0.28	0.25	0.19	0.13	0.25	0.18	0.36	0.26	0.29
L.O.I.	1.68	2.12	1.88	2.60	3.52	4.17	5.99	3.92	3.14	2.72	3.54	2.86	3.29
Total	100.00	100.00	100.00	100.00	99.99	99.94	100.09	100.08	100.01	100.09	100.08	99.98	100.01
Mg#	75.1	67.2	71.2	78.0	71.2	69.4	71.0	46.1	55.5	67.0	69.7	59.3	62.9
Zn	20	54	41	9	107	80	100	208	83	99	97	100	81
Ni	198	134	146	176	91	103	86	139	60	118	85	66	85
Co	36	34	33	36	41	31	38	46	39	45	40	34	36
Cr	314	182	327	358	198	197	160	22	131	79	191	118	165
V	185	274	198	205	256	264	179	503	255	270	253	283	284
Rb	3	<d.l.	2	<d.l.	7	4	21	22	81	4	16	38	<d.l.
Ba	40	23	31	30	<d.l.	<d.l.	60	153	98	67	30	51	34
Pb	4	6	5	<d.l.	5	9	2	<d.l.	<d.l.	3	2	7	6
Sr	197	234	201	284	160	127	209	292	33	54	172	172	63
Zr	117	185	130	123	172	162	123	192	119	62	225	380	225
Y	23	38	25	23	42	41	27	67	36	39	33	47	40
ICP-MS analyses:													
Sc	27.5	41.5	24.0	24.8	29.2	27.3	24.1	67.0	24.2	37.8	31.9	25.7	29.1
La	2.65	4.14	2.58	2.48	4.81	3.70	3.73	5.27	4.65	4.38	8.53	13.5	4.04
Ce	8.67	14.0	8.43	7.88	16.4	12.9	11.6	16.92	15.19	13.9	22.9	34.0	13.4
Pr	1.57	2.49	1.46	1.36	3.03	2.48	1.99	3.28	2.92	2.68	3.53	4.93	2.30
Nd	8.98	14.6	8.30	7.54	15.5	12.8	11.2	17.22	15.26	14.4	18.0	23.2	12.5
Sm	2.98	4.96	2.54	2.35	4.64	3.89	3.52	5.86	5.22	4.89	5.43	6.77	4.04
Eu	1.20	1.59	0.96	0.90	1.46	1.21	1.17	1.85	1.73	1.46	1.68	2.01	1.51
Gd	3.99	6.20	3.01	2.93	4.48	3.69	4.50	7.29	6.64	6.18	5.25	6.70	5.25
Tb	0.71	1.11	0.51	0.52	0.79	0.65	0.74	1.25	1.14	1.05	0.92	1.15	0.93
Dy	4.75	7.59	3.40	3.45	5.22	4.06	4.77	7.86	7.17	6.68	6.04	7.45	5.73
Ho	1.02	1.53	0.72	0.72	1.06	0.87	0.93	1.62	1.49	1.30	1.20	1.49	1.15
Er	2.85	4.43	2.01	2.06	2.91	2.31	2.50	4.07	3.94	3.41	3.28	4.00	3.29
Tm	0.43	0.68	0.30	0.31	0.42	0.34	0.35	0.54	0.53	0.49	0.41	0.55	0.49
Yb	2.70	4.48	1.98	1.97	2.59	2.10	2.12	3.08	2.97	2.82	2.35	3.15	3.12
Lu	0.38	0.62	0.27	0.28	0.37	0.29	0.26	0.39	0.37	0.35	0.27	0.39	0.43
Nb	2.07	1.63	1.88	1.27	3.23	2.69	5.94	6.97	5.99	3.73	3.67	7.26	1.71
Hf	2.17	3.87	2.19	1.89	3.62	3.15	3.06	4.18	3.24	3.11	4.69	4.28	3.50
Ta	0.14	0.14	0.11	0.08	0.17	0.16	0.41	0.60	0.26	0.12	0.17	0.38	0.18
Th	0.08	0.12	0.08	0.05	0.14	0.11	0.18	0.21	0.19	0.15	0.15	0.42	0.11
U	0.03	0.04	0.03	0.02	0.06	0.04	0.08	0.12	0.06	0.03	0.07	0.12	0.05
Zr/Y	5.07	4.87	5.23	5.25	4.13	3.92	4.55	2.86	3.30	1.60	6.79	8.02	5.62
Nb/Y	0.09	0.04	0.08	0.05	0.08	0.07	0.22	0.14	0.17	0.10	0.11	0.15	0.04
$(La/Sm)_N$	0.57	0.54	0.66	0.68	0.67	0.61	0.68	0.58	0.58	0.58	1.10	1.29	0.65
$(Sm/Yb)_N$	1.23	1.23	1.43	1.33	1.99	2.06	1.84	2.11	1.95	1.93	2.57	2.39	1.44
$(La/Yb)_N$	0.70	0.66	0.93	0.90	1.33	1.26	1.26	1.23	1.12	1.11	2.61	3.08	0.93
$(Dy/Yb)_N$	1.18	1.13	1.15	1.17	1.35	1.29	1.51	1.71	1.62	1.59	1.72	1.58	1.23

Table 2 (*continued*)

					Upper Schistes Lustrés									
Unit	SPT	Inz.-type	Inz.-type	Inz.-type	Inz.-type	Inz.-type	Inz.-type	Inz.-type	Inz.-type	Inz.-type	SAT	SAT	SAT	SAT
Locality	Colle S. Stefano	Santa Maria	Santa Maria	Santa Maria	Vescovato	Alesani	Alesani	Linguizzeta	Tox	Tox	Mt. St. Angelo	Mt. St. Angelo	Mt. St. Angelo	Mt. St. Angelo
Sample	CO17	CO109	CO112	CO113	CO52V	CO61	CO62	CO64T	CO71T	CO73T	CO105A	CO106A	CO107A	CO108A
Rock	Bls	Met-Bas	Met-Bas	Met-Bas	Bls	Met-Bas	Met-Bas	Met-Bas	Met-Bas	Met-Bas	Met-Bas	Met-Bas	Met-Bas	Met-B.And
Note	n.d.	n.d.	n.d.	n.d.	Pillow	Pillow	Pillow	Pillow	Pillow	n.d.	n.d.	n.d.	n.d.	n.d.
XRF analyses:														
SiO_2	46.77	50.47	47.35	49.01	48.18	48.33	45.76	47.63	46.42	48.50	49.86	50.01	51.76	53.39
TiO_2	2.43	1.37	1.37	1.58	1.91	1.35	1.30	1.34	1.43	1.08	1.64	1.63	1.64	2.15
Al_2O_3	15.98	15.23	17.18	16.77	13.94	15.96	17.22	15.32	16.73	16.28	15.54	14.74	14.41	13.60
Fe_2O_3	1.42	1.19	1.19	1.21	1.39	1.15	1.09	1.16	1.04	0.91	1.17	1.10	1.09	1.19
FeO	9.46	7.91	7.90	8.09	9.28	7.66	7.24	7.75	6.91	6.04	7.82	7.34	7.26	7.96
MnO	0.18	0.13	0.14	0.17	0.15	0.15	0.20	0.15	0.09	0.09	0.17	0.19	0.15	0.14
MgO	8.92	7.16	5.07	7.84	7.35	7.94	8.23	8.00	10.59	10.40	8.54	9.76	7.63	5.45
CaO	6.39	7.93	10.39	6.38	9.03	7.80	10.13	9.86	7.82	7.47	7.40	7.25	8.57	8.27
Na_2O	3.96	4.01	4.02	3.14	3.13	3.88	2.96	3.52	3.15	3.65	4.79	4.04	4.81	5.98
K_2O	0.82	0.69	0.15	1.79	0.28	0.46	0.37	0.05	0.11	0.33	0.13	0.47	0.20	0.13
P_2O_5	0.35	0.19	0.23	0.22	0.40	0.30	0.39	0.38	0.32	0.29	0.24	0.23	0.25	0.31
L.O.I.	3.53	3.66	5.04	3.77	4.93	5.06	5.11	4.92	5.27	4.89	2.68	3.18	2.24	1.48
Total	100.21	99.91	100.03	99.95	99.98	100.05	99.99	100.07	99.90	99.94	99.97	99.95	100.01	100.06
Mg#	62.7	61.7	53.4	63.3	58.5	64.9	67.0	64.8	73.2	75.4	66.1	70.3	65.2	54.9
Zn	110	75	79	81	94	78	83	65	64	45	74	74	66	81
Ni	75	98	116	111	105	118	121	118	112	107	96	91	86	84
Co	40	31	37	42	39	42	37	36	30	33	33	31	30	36
Cr	124	386	435	300	226	353	328	214	285	332	219	217	232	135
V	278	243	246	276	297	232	228	235	245	200	269	248	242	295
Rb	18	16	2	32	9	11	8	3	4	5	2	11	5	<d.l.
Ba	32	10	14	46	35	52	32	46	48	65	<d.l.	10	<d.l.	22
Pb	4	5	8	<d.l.	2	6	4	2	5	8	<d.l.	5	7	7
Sr	209	77	122	60	176	120	104	219	172	261	67	88	140	118
Zr	370	99	107	129	231	146	142	131	192	160	152	147	142	202
Y	49	31	37	39	46	29	27	29	32	25	38	37	36	45
ICP-MS analyses:														
Sc	27.8	24.7	31.2	34.1	33.9	32.7	34.7	35.0	42.2	43.4	27.0	23.7	26.3	28.1
La	13.54	2.28	3.37	3.73	6.08	4.45	3.94	2.15	2.75	3.15	4.48	3.21	3.54	4.94
Ce	35.9	7.81	11.2	13.0	18.0	14.0	12.6	7.54	9.86	10.6	13.9	10.9	11.1	16.2
Pr	5.04	1.44	1.85	2.20	2.99	2.39	2.12	1.35	1.79	1.84	2.39	1.97	1.93	2.86
Nd	24.6	8.23	9.76	11.6	15.1	11.7	11.0	7.68	9.49	9.35	12.1	9.67	9.67	15.0
Sm	6.62	2.77	3.11	3.99	4.71	3.57	3.45	2.94	3.42	3.34	3.59	3.03	3.01	4.66
Eu	2.06	0.95	1.14	1.31	1.45	1.22	1.27	1.15	1.16	1.25	1.19	0.95	1.02	1.45
Gd	6.79	3.57	3.85	4.66	5.14	3.97	3.99	3.96	4.51	3.99	4.17	3.48	3.75	5.68
Tb	1.20	0.66	0.68	0.78	0.90	0.71	0.70	0.77	0.82	0.72	0.75	0.62	0.65	1.00
Dy	7.78	4.10	4.42	5.21	6.03	4.64	4.72	5.05	5.32	4.61	4.71	3.92	4.35	6.35
Ho	1.56	0.87	0.87	1.08	1.21	0.94	0.97	1.07	1.09	0.99	1.00	0.82	0.92	1.34
Er	4.36	2.45	2.51	2.93	3.23	2.64	2.57	3.03	3.08	2.75	2.71	2.29	2.44	3.61
Tm	0.53	0.35	0.36	0.41	0.44	0.38	0.36	0.45	0.48	0.42	0.37	0.31	0.34	0.51
Yb	3.11	2.29	2.24	2.57	2.67	2.30	2.19	2.91	3.01	2.74	2.28	1.86	2.09	2.92
Lu	0.35	0.31	0.28	0.31	0.36	0.30	0.28	0.38	0.37	0.39	0.32	0.23	0.28	0.39
Nb	6.68	1.59	1.17	1.71	2.52	2.47	2.28	1.83	1.27	1.61	2.08	1.87	2.08	3.04
Hf	5.98	2.23	2.31	2.59	3.66	2.71	2.81	2.28	2.74	2.25	3.84	2.37	3.50	4.54
Ta	0.37	0.19	0.14	0.16	0.21	0.18	0.22	0.20	0.21	0.18	0.13	0.11	0.14	0.15
Th	0.45	0.10	0.11	0.12	0.18	0.21	0.19	0.07	0.08	0.08	0.13	0.13	0.14	0.17
U	0.15	0.05	0.06	0.03	0.04	0.08	0.06	0.06	0.03	0.04	0.05	0.03	0.04	0.05
Zr/Y	7.59	3.19	2.91	3.33	5.07	5.08	5.16	4.53	6.02	6.29	4.04	3.95	3.95	4.45
Nb/Y	0.14	0.05	0.03	0.04	0.06	0.09	0.08	0.06	0.04	0.06	0.06	0.05	0.06	0.07
$(La/Sm)_N$	1.32	0.53	0.70	0.60	0.83	0.81	0.74	0.47	0.52	0.61	0.81	0.68	0.76	0.68
$(Sm/Yb)_N$	2.36	1.34	1.54	1.72	1.96	1.72	1.75	1.12	1.26	1.35	1.75	1.81	1.60	1.77
$(La/Yb)_N$	3.12	0.72	1.08	1.04	1.63	1.39	1.29	0.53	0.65	0.82	1.41	1.24	1.21	1.21
$(Dy/Yb)_N$	1.67	1.20	1.32	1.35	1.51	1.35	1.44	1.16	1.18	1.13	1.38	1.41	1.39	1.46

Table 2 (*continued*)

Unit	Eclogite		Lower Schistes Lustrés											
Locality	Volpajola Accendi Pipa	Volpajola Accendi Pipa	Castag. Lancone	Castag. Lancone	Castag. Lancone	Castag. Quarceto	Castag. Volpajola	Castag. Bucotaggio	Castag. Cervione	Castag. Santa Maria	Castag. S.Andrea di Cotone	Castag. S.Andrea di Cotone	Castag. Matra	Castag. Matra
Sample	CO133AP	CO136AP	CO19L	CO21L	CO22L	CO26G	CO28G	CO57	CO59	CO116	CO117	CO60	CO65M	CO68M
Rock	eclogite	eclogite	Bls	Bls	Bls	Bls	Bls	Bls	Bls	Met-Bas	Met-And	Bls	Bls	Bls
Note	n.d.	n.d.	n.d.	n.d.	n.d.	n.d.	n.d.	pillow	pillow	n.d.	n.d.	n.d.	n.d.	n.d.
XRF analyses:														
SiO_2	50.16	49.60	45.60	46.79	45.63	49.49	48.92	44.99	46.57	46.77	56.29	49.17	46.58	48.65
TiO_2	1.91	1.81	1.28	2.02	1.25	1.26	2.20	1.13	1.26	1.64	0.35	1.63	1.68	1.58
Al_2O_3	13.93	15.31	15.45	14.80	14.91	17.98	13.33	13.28	17.08	16.59	16.75	15.67	14.88	12.81
Fe_2O_3	1.37	1.51	1.15	1.47	1.20	1.21	1.54	1.45	1.03	1.25	0.28	1.29	1.30	1.19
FeO	9.12	10.05	7.63	9.82	8.02	8.08	10.26	9.69	6.88	8.34	1.84	8.63	8.67	7.91
MnO	0.15	0.13	0.22	0.13	0.15	0.16	0.18	0.16	0.24	0.13	0.07	0.14	0.17	0.19
MgO	7.13	6.08	12.27	10.73	7.99	6.73	8.84	5.99	10.09	4.96	7.57	7.10	8.05	9.16
CaO	9.15	8.37	8.02	7.11	11.27	6.29	8.14	12.48	7.13	10.58	5.09	6.72	9.65	10.11
Na_2O	3.85	2.89	2.82	3.67	3.20	2.93	3.14	4.25	2.30	3.89	5.86	4.10	3.55	2.99
K_2O	0.38	1.62	0.11	0.02	0.50	2.48	0.93	0.11	1.84	0.08	0.28	0.79	0.38	0.08
P_2O_5	0.25	0.18	0.27	0.29	0.39	0.22	0.32	0.44	0.25	0.25	0.05	0.28	0.40	0.43
L.O.I.	2.67	2.37	5.17	3.17	5.43	3.08	2.21	6.03	5.28	5.56	5.48	4.43	4.72	4.81
Total	100.06	99.92	99.99	100.02	99.94	99.90	100.02	100.00	99.95	100.03	99.91	99.95	100.03	99.89
Mg#	58.2	51.9	74.1	66.1	64.0	59.8	60.6	52.4	72.3	51.4	88.0	59.5	62.3	67.4
Zn	106	92	43	101	70	98	122	106	117	74		83	80	76
Ni	86	97	86	91	88	72	78	66	130	134	3	101	91	106
Co	44	35	31	41	39	42	44	35	30	39	1	32	34	33
Cr	107	186	394	232	402	355	227	186	394	423	4	244	191	227
V	295	236	250	304	240	252	337	214	225	226	20	244	254	245
Rb	12	37	2	2	6	46	24	6	35	2	<d.l.	17	10	2
Ba	77	96	23	29	30	67	52	54	70	37	<d.l.	41	62	24
Pb	<d.l.	2	3	5	<d.l.	3	5	3	3	3	13	<d.l.	5	<d.l.
Sr	151	210	111	84	174	202	100	180	70	71	26	95	204	145
Zr	103	129	115	195	114	132	234	129	124	129	156	207	190	184
Y	38	36	27	42	25	28	47	27	28	34	27	40	34	33
ICP-MS analyses:														
Sc	37.4	40.4	28.9	32.1	38.9	31.7	33.8	23.7	33.6	29.5	37.4	28.3	33.8	38.8
La	5.22	4.10	2.91	5.07	2.67	2.14	6.08	3.95	2.96	2.06	3.74	3.18	3.35	3.61
Ce	16.5	13.1	9.78	17.0	8.29	7.04	19.9	12.4	9.30	6.59	11.7	11.2	11.5	12.3
Pr	2.98	2.38	1.72	2.88	1.48	1.41	3.45	2.03	1.68	1.33	1.96	2.03	2.02	2.18
Nd	17.0	13.7	9.37	14.2	8.57	7.67	18.3	10.2	9.00	7.66	9.65	10.7	10.9	11.7
Sm	5.35	4.63	3.14	4.75	3.05	2.89	5.88	3.31	3.05	2.76	3.24	3.82	3.86	4.14
Eu	1.65	1.47	1.09	1.53	1.21	1.11	1.73	1.29	1.06	1.01	1.19	1.43	1.47	1.47
Gd	6.75	5.92	3.95	5.41	4.30	3.94	6.60	4.15	3.51	3.75	3.89	5.29	5.02	5.10
Tb	1.14	1.04	0.69	0.94	0.80	0.73	1.15	0.72	0.61	0.71	0.66	0.97	0.94	0.92
Dy	7.34	6.88	4.62	6.61	5.43	4.65	7.69	4.54	4.02	4.54	4.37	6.27	6.22	5.91
Ho	1.50	1.44	0.97	1.41	1.18	0.92	1.65	0.92	0.85	0.97	0.89	1.31	1.30	1.22
Er	4.20	4.07	2.73	3.98	3.25	2.57	4.73	2.55	2.27	2.83	2.53	3.66	3.57	3.35
Tm	0.57	0.55	0.40	0.59	0.48	0.37	0.67	0.38	0.32	0.42	0.34	0.55	0.55	0.48
Yb	3.50	3.32	2.47	3.59	2.92	2.25	3.85	2.43	1.90	2.68	2.14	3.23	3.32	2.81
Lu	0.47	0.43	0.31	0.45	0.38	0.28	0.45	0.31	0.23	0.35	0.27	0.40	0.40	0.36
Nb	2.53	2.18	1.99	2.88	1.58	1.33	3.22	1.31	1.66	1.96	1.63	1.48	1.64	2.14
Hf	2.96	3.01	2.29	3.30	3.06	2.36	4.28	2.43	2.64	2.24	1.51	3.17	2.72	3.54
Ta	0.30	0.21	0.17	0.19	0.12	0.19	0.24	0.16	0.16	0.14	0.15	0.17	0.19	0.18
Th	0.25	0.22	0.09	0.17	0.10	0.12	0.21	0.22	0.18	0.10	0.10	0.12	0.09	0.11
U	0.07	0.08	0.03	0.05	0.03	0.08	0.06	0.12	0.06		0.08	0.06	0.15	0.05
Zr/Y	2.72	3.57	4.31	4.68	4.55	4.73	5.02	4.78	4.50	3.79	5.78	5.15	5.65	5.56
Nb/Y	0.07	0.06	0.07	0.07	0.06	0.05	0.07	0.05	0.06	0.06	0.06	0.04	0.05	0.06
$(La/Sm)_N$	0.63	0.57	0.60	0.69	0.56	0.48	0.67	0.77	0.63	0.48	0.74	0.54	0.56	0.56
$(Sm/Yb)_N$	1.70	1.55	1.42	1.47	1.16	1.43	1.70	1.51	1.78	1.15	1.68	1.31	1.29	1.64
$(La/Yb)_N$	1.07	0.89	0.85	1.01	0.65	0.68	1.13	1.17	1.12	0.55	1.25	0.71	0.72	0.92
$(Dy/Yb)_N$	1.40	1.39	1.25	1.23	1.24	1.38	1.34	1.25	1.42	1.13	1.37	1.30	1.26	1.41

(LILE) (e.g., Pearce, 1983). Nonetheless, primary magmatic relationships are commonly preserved by those elements that are considered relatively immobile during alteration and metamorphism (e.g., Beccaluva et al., 1979; Pearce and Norry, 1979; Shervais, 1982), i.e., high field strength elements (HFSE) (e.g., Ti, P, Zr, Y, Sc, Nb, Ta, Hf, Th), some transition metals (e.g., Ni, Co, Cr, V), and the REE. In fact, variable amounts of LILE mobilization have been recognized in the studied rocks when observing the relative variation of these elements with respect to many immobile elements (not shown herein) and therefore they are not used in the geochemical discussion presented in this paper. In some circumstances, such as the extensive carbonatization of metabasites, the light REE (LREE) can be mobilized. Car-

bonate-rich samples were excluded from this study and the good correlations (e.g., r^2 for La vs. Zr = 0.90; r^2 for Ce vs. Zr = 0.92) between these elements and many immobile elements (not shown) indicate that LREE mobilization during alteration and metamorphism was negligible. Thus, as they appear to act isochemically during metamorphism, HFSE, transition metals and REE have been utilized to determine the petrogenetic features of Corsica metabasites and to investigate the variations in mantle source composition (mantle heterogeneities) and melting, as well as low-pressure fractionation processes.

Geochemical classification and general features

Viewed overall, the chemistry of basaltic and metabasaltic rocks from the different Corsica ophiolitic units (Table 2) displays many common geochemical characteristics. The general sub-alkaline, tholeiitic nature of these rocks is testified by the low Nb/Y ratio (0.03 - 0.68), as well as by the Ti/V ratio (25 - 55), which are in the range for high-Ti tholeiitic basalts from mid-ocean ridge settings (Shervais, 1982). Volcanic and metavolcanic rocks from the various ophiolitic units range in composition from basalt to basaltic andesite and Fe-basalt, having SiO_2 ranging from 43.22 to 55.02 wt%. Basalts are volumetrically predominant, while basaltic andesites and Fe-basalts are subordinate. Only one sample from the LSL unit (CO117) is a metaandesite. MgO abundances in all samples range from 4.67 to 13.90 wt%. Variations of selected major and trace elements vs. Zr (used here as a differentiation index) are presented in Fig. 2. Although there is some tendency for samples from the same ophiolitic unit, notably the Balagne, Sant'Angelo di Tenda, Inzecca, and other Inzecca-type units to plot as groups, all samples show incompatible element (TiO_2, P_2O_5, Y, Nb) increase with increasing Zr. By contrast, Cr displays a marked decrease with increasing Zr. FeO_t display the typical tholeiitic trend; that is, iron increase from the less to the moderately evolved basalts followed by a decrease toward the more evolved basalts and basaltic andesites. P_2O_5 contents are relatively high in metabasaltic rocks, ranging from 0.14 to 0.48 wt%. In the meta-Fe-basalts P_2O_5 may either be very high (0.55-0.90wt%) or very low (0.03-0.05 wt%), likely depending on the amount of apatite crystallization in the various stages of the fractionation processes.

Although the general compositional features of basalts and metabasalts from the various ophiolitic units of Corsica point out for a common genesis in a mid-ocean ridge setting, they can be geochemically distinguished on the bases of their HFSE and REE composition, as illustrated in the next section and Summarized in Table 3.

Geochemical variability of volcanic and metavolcanic rocks from the ophiolitic units of Corsica

Balagne Unit

The Balagne samples are mainly represented by poorly fractionated basalts (Mg# = 60.9-70.5) [Mg# = molar ratio of MgO / (MgO + FeO) * 100], though basaltic andesites are subordinately found. HFSE and REE composition of the Balagne samples are plotted in Fig. 3a, b. N-MORB normalized (Sun and McDonough, 1989) HFSE show flat, slightly enriched patterns. Samples from the lower part of the volcanic sequence (e.g., CO119B, CO120B) have no Ta depletion relative to Th, whereas samples from the top of the vol-

canic sequence (e.g., CO138B, CO139B), have a little Ta/Th depletion (Fig. 3a). This aspect is also evidenced in the diagram of Fig. 4. The Balagne basalts display chondrite normalized (Sun and McDonough, 1989) patterns significantly different from both N- and E-MORB (Fig. 3b). In fact, they are slightly enriched in LREE with respect to heavy REE (HREE), as exemplified in Table 3. Nonetheless, LREE are variably depleted with respect to medium REE (MREE), with (La/Sm)$_N$ ratios ranging from 0.97 to 0.99 for samples from the base of the volcanic sequence and from 0.55 to 0.73 for samples from the top of the volcanic sequence. In Fig. 4, the Balagne basalts plot between the compositions of N- and E-MORB. Basalts from the Balagne Unit have previously been interpreted as T-MORBs generated during the onset of the oceanic spreading (Venturelli et al., 1979). However, the incompatible element composition of basalts from the top of the volcanic sequence suggests that these rocks are more similar to N-MORBs than to T-MORBs. By contrast, basalts from the bottom of the volcanic sequence display slightly enriched chemical features, though some ambiguity in their definition still remain. In addition, the Balagne basalts have previously been considered as correlative of the External Liguride basalts of the Northern Apennine. In fact, these two ophiolitic series show very similar incompatible element composition (Fig. 3a), but significantly differ in the REE content (Fig. 3b).

Nebbio Unit

The Nebbio samples are represented by basalts and basaltic andesites, which cover a wide range of fractionation (Mg# = 54.2-70.0). N-MORB normalized (Sun and McDonough, 1989) HFSE show slightly enriched patterns (Fig. 3c). A Nb negative anomaly can be observed for samples CO1N and CO4N, whereas all samples display a Zr positive anomaly. The chondrite normalized (Sun and McDonough, 1989) REE compositions display patterns slightly enriched in LREE with respect to HREE (Fig. 3d, Table 3). Moreover, LREE are slightly depleted with respect to MREE (Table 3). Except for the LREE compositions, they show REE patterns similar to those of typical E-MORB from modern oceanic settings (Fig. 3d). In Fig. 4, the Balagne basalts plot between the compositions of N- and E-MORB. In summary, of more significance is the mild enrichment of the LREE, Ta and Th shown by the Nebbio basalts, which can thus be classified as T-MORBs. The Nebbio basalts, similarly to the Balagne basalts, have previously been considered as correlative of the External Liguride basalts of the Northern Apennine. The data presented herein are in contrast with this conclusion since basalts from the External Ligurides are generally more depleted in Th, Nb and LREE (Fig. 3c, d).

Rio Magno Unit

The Rio Magno samples are represented by relatively unfractionated basalts (Mg# = 64.2-74.5). Spiderdiagrams of Fig. 3e evidence HFSE flat patterns, which are similar to those of typical N-MORB, as well as to N-MORB from the Internal Ligurides of the Northern Apennine (Fig. 3e, f). All samples display a mild Nb negative anomaly and many samples have Zr positive anomalies. REE patterns normalized to chondrite (Sun and McDonough, 1989) show N-MORB characteristics with LREE slightly depleted patterns (Fig. 3f, Table 3). In Fig. 4, the Rio Magno basalts have Th/Yb and Ta/Yb ratios very similar to that of the typical N-MORB (Sun and McDonough, 1989).
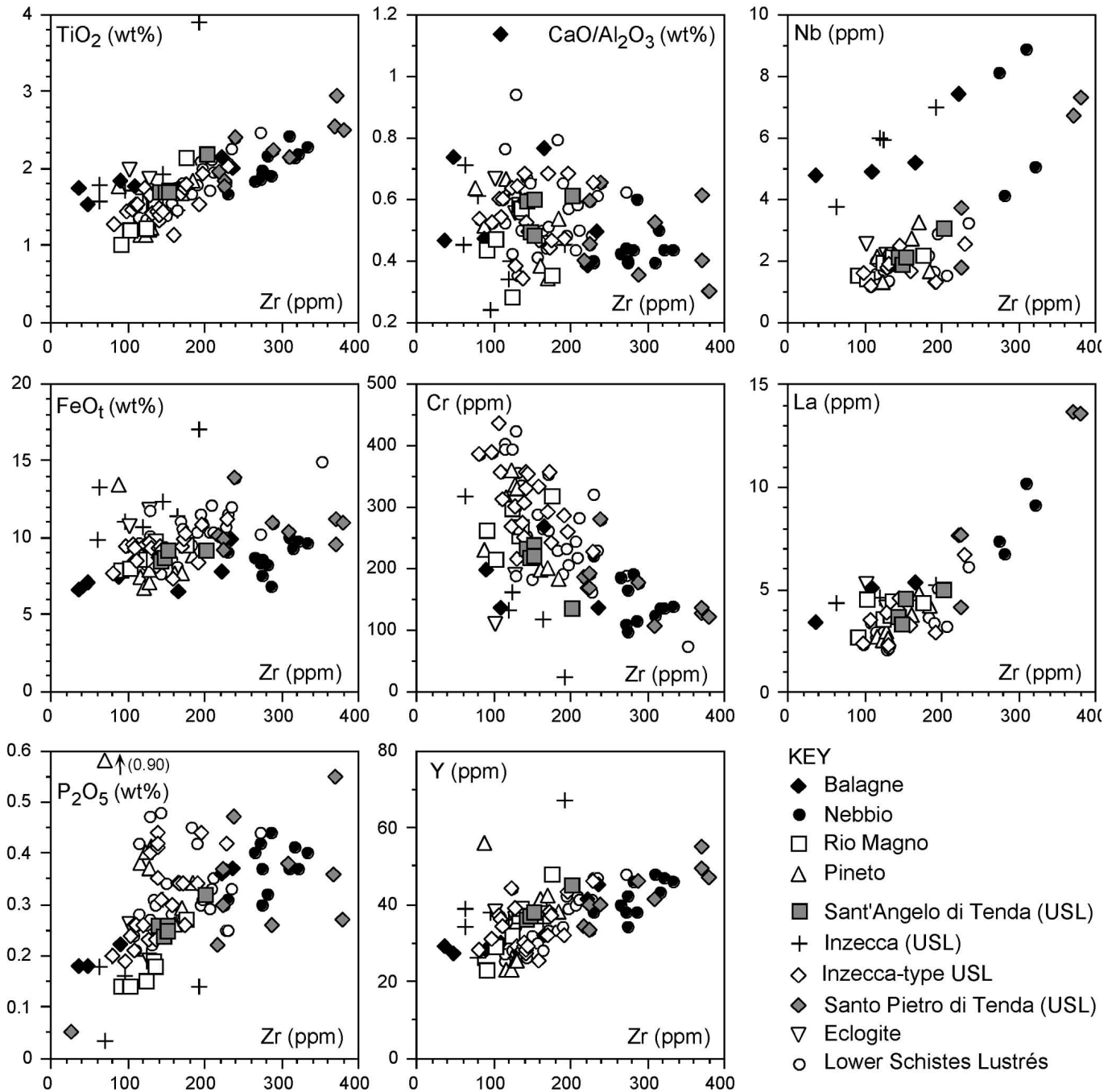
Fig. 2 - Variation of selected major and trace elements vs. Zr for volcanic and metavolcanic rocks from Corsica ophiolites.

Pineto Unit

The Pineto samples include basaltic dykes cross-cutting the gabbro sequence (Saccani et al., 2000) and basalts stratigraphically overlaying gabbros. All these rocks are relatively uniform in composition (Table 2) and poorly fractionated (Mg# = 67.2-78.0). A MORB-like composition of Pineto basalts has already been suggested by Saccani et al. (2000). The incompatible element diagram of Fig. 3g shows that HFSE display a MORB pattern, although P and Zr appear to be slightly enriched. Of more significance is the depletion of Th, U, Ta, and, to a lesser extent, Nb relative to the other HFSE. The chondrite-normalized REE patterns of the Pineto Massif basalts differ from those of typical N-MORBs in that most of them show marked HREE/MREE fractionation

(Fig. 3h), as exemplified by the high $(Sm/Yb)_N$ ratios (Table 3). The low $(La/Sm)_N$ ratios (Table 3) are however similar to those of N-MORBs. The slightly negative anomaly in Eu displayed by the more evolved samples (e.g. CO40P) is consistent with the accumulation of plagioclase observed in the associated intrusive sequence (Saccani et al., 2000).

Upper Schistes Lustrés of the Sant'Angelo di Tenda Unit

Metabasites from the Sant'Angelo di Tenda Unit are basaltic to basaltic andesitic in composition (Table 2). Their variable Mg# (54.9-70.3) suggest that they represent variably differentiated products.

The most striking geochemical features are rather flat patterns from La to Y, but Th, Ta, Nb depletion and P, Zr

Table 3. Summary of the geochemical affinity and variation of some chondrite-normalized (Sun and McDonough, 1989) REE ratios for volcanic and metavolcanic rocks from the main ophiolitic units of the Alpine Corsica.

Unit	Affinity	$(La/Sm)_N$		$(Sm/Yb)_N$		$(La/Yb)_N$	
		range	mean ± std. dev.	range	mean ± std. dev.	range	mean ± std. dev.
Balagne							
bottom	T-MORB	0.97-0.99	0.98 ± 0.02	1.66-1.78	1.72 ± 0.09	1.60-1.77	1.68 ± 0.12
top	N-MORB	0.55-0.73	0.64 ± 0.13	1.99-2.06	2.02 ± 0.04	1.09-1.50	1.30 ± 0.29
Nebbio	T-MORB	0.81-1.02	0.90 ± 0.10	1.39-1.81	1.59 ± 0.21	1.13-1.76	1.44 ± 0.33
R.Magno	N-MORB	0.57-0.68	0.60 ± 0.03	1.39-2.28	1.62 ± 0.44	0.80-1.33	0.97 ± 0.24
Pineto	N-MORB	0.54-0.68	0.62 ± 0.06	1.23-2.06	1.54 ± 0.38	0.66-1.33	0.97 ± 0.28
Sant'Angelo di Tenda (USL)	N-MORB	0.68-0.81	0.73 ± 0.06	1.60-1.81	1.73 ± 0.09	1.21-1.41	1.27 ± 0.09
Inzecca (USL)	N-MORB	0.58-0.68	0.60 ± 0.05	1.84-2.11	1.96 ± 0.11	1.11-1.26	1.18 ± 0.07
Inzecca-type (USL)	N-MORB	0.47-0.90	0.65 ± 0.14	1.12-1.96	1.53 ± 0.28	0.53-1.63	1.03 ± 0.40
Santo Pietro di Tenda (USL)	T-MORB	0.99-1.32	1.17 ± 0.24	2.36-2.57	2.44 ± 0.12	2.30-3.12	2.83 ± 0.46
Castagniccia (LSL)	N-MORB	0.47-0.77	0.61 ± 0.10	1.15-1.70	1.46 ± 0.21	0.55-1.13	0.90 ± 0.24
Eclogite (LSL)	N-MORB	0.57-0.63	0.60 ± 0.04	1.55-1.70	1.63 ± 0.11	0.89-1.07	0.98 ± 0.13

Abbreviations, USL: Upper Schistes Lustrés; LSL: Lower Schistes Lustrés; T-MORB: transitional-type mid-ocean ridge basalt; N-MORB: normal-type mid-ocean ridge basalt.

enrichment relative to the other HFSE (Fig. 5a). The chondrite-normalized REE patterns are slightly depleted in the LREE with respect to the medium REE (Fig. 5b, Table 3). Although HREE are slightly fractionated with respect to LREE and MREE (Table 3), the Th and Nb contents, as well as the overall REE composition generally resembling those observed in N-MORBs. A close similarity in HFSE compositions with respect to the N-MORB from the Internal Ligurides is observed (Fig. 5a, b).

Upper Schistes Lustrés of the Inzecca Unit

The Inzecca Unit metabasites include dykes cutting the metagabbro sequence (e.g., samples CO122PC, CO123PC), and samples from different levels of the volcanic sequence. They range in composition from basalt to Fe-basalt (Table 2). HFSE generally display patterns, which are similar to those of typical N-MORB (Fig. 5c). However, some samples display Th, U, Ta, and Zr depletion, whereas dykes cutting the metagabbro sequence have Ta enrichment. REE patterns show LREE/MREE depletion and mild HREE fractionation with respect to MREE (Fig. 5d, Table 3). In Fig. 4, metabasites from the volcanic sequence have Th/Yb and Ta/Yb ratios very similar to those of the typical N-MORB, whereas dykes in the metagabbro sequence have comparatively high Ta/Yb ratios. In addition, the Inzecca metabasaltic rocks display similar REE composition with respect to the N-MORB from the Internal Ligurides (Fig. 5c, d).

Upper Schistes Lustrés of the Inzecca-type units

Metabasites from these USL units have basaltic composition with highly variable Mg# (Table 2). They show quite similar N-MORB normalized HFSE patterns (Fig. 5e, g) and

no differences can be observed between blueschists and greenschist-facies metabasites. These USL metabasites display relatively flat patterns, with Nb, and to a lesser extent, Th depletion with respect to other HFSE (Fig. 5e, g). All samples from the various Inzecca-type units have pronounced P and Zr positive anomalies. The chondrite-normalized REE patterns show very similar HREE compositions, but variable degrees of LREE enrichment (Fig. 5f, h, Table 3). They also show a mild HREE fractionation with respect to MREE, with $(Sm/Yb)_N$ = 1.12 - 1.96. In summary, the HFSE and REE composition of these samples is generally compatible with N-MORB composition.

Upper Schistes Lustrés of the Santo Pietro di Tenda Unit

Metabasites from this unit have basaltic composition with variable Mg# (Table 2). Only one of the studied samples (CO43) shows Th and Nb depletion with respect other HFSE (Fig. 5i) and pronounced Zr positive anomaly. The chondrite-normalized REE pattern of CO43 (Fig. 5j) shows LREE/MREE depletion with $(La/Sm)_N$ of 0.65. Likewise other USL and LSL metabasites, this sample also show a mild HREE fractionation with respect to MREE, with $(Sm/Yb)_N$ = 1.44. The HFSE and REE composition of this sample is compatible with N-MORB composition. By contrast, all the other samples from the Santo Pietro di Tenda Unit do not display any Th, Ta, and Nb depletion (Fig. 5i) and have LREE enriched pattern and marked HREE fractionation with respect to LREE and MREE (Fig. 5j, Table 3). The HFSE and REE characteristics of this sample are compatible with T-MORB composition.

*Lower Schistes Lustrés of the Castagniccia Unit*

Metabasites from the LSL unit cover a wide range of
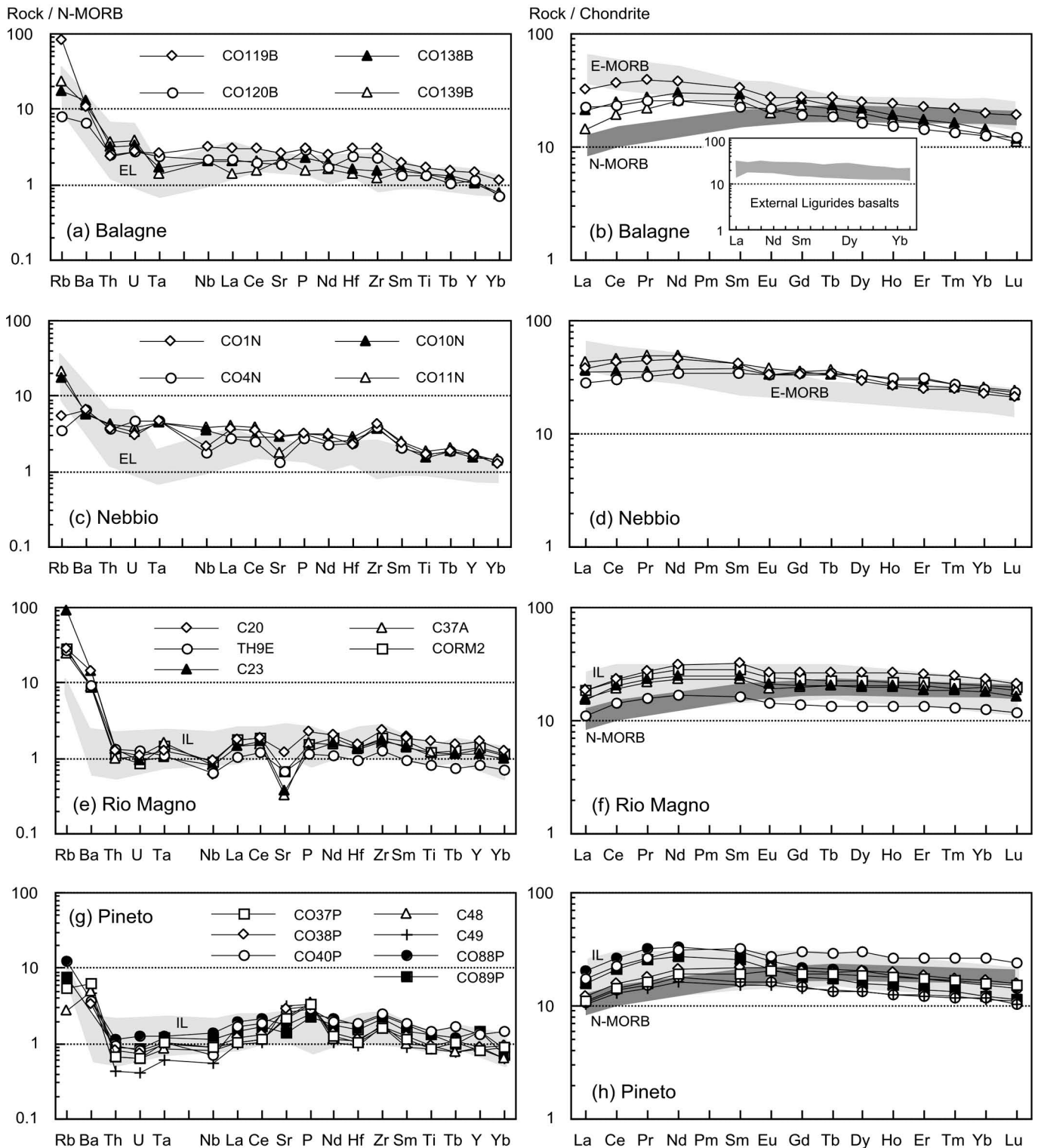
Fig. 3 - N-MORB normalized incompatible element and chondrite-normalized REE patterns for volcanic rocks from the Balagne (a, b), Nebbio (c, d), Rio Magno (e, f) and Pineto (g, h) Units. Normalizing values are from Sun and McDonough (1989). Compositional variation (gray fields) of ophiolitic basalts from the External Ligurides (EL) of Northern Apennine (data from: Vannucci et al., 1993; Marroni et al., 1998; Montanini et al., 2008), ophiolitic basalts from the Internal Ligurides (IL) of Northern Apennine (data from: Venturelli et al., 1981; Ottonello et al., 1984; Cortesogno and Gaggero, 1992), as well as normal-type mid-ocean ridge basalts (N-MORB) and enriched-type mid-ocean ridge basalts (E-MORB) from modern oceanic settings (data from: Le Roex, 1987) are reported for comparison.

compositions, from basalt to andesite (Table 3). In general, very little differences in HFSE contents can be observed in samples from different localities (Table 2) and no differences can be observed between blueschists and metabasites in the greenschist-facies. Most of the samples are generally typified by relatively flat N-MORB normalized HFSE patterns (Fig. 6a, c). Some samples have Th and Nb depletion. The metaandesite CO117 is characterized by marked negative anomalies in P and Ti (Fig. 6c), which are probably related to early crystallization of apatite and Fe-Ti-oxides.
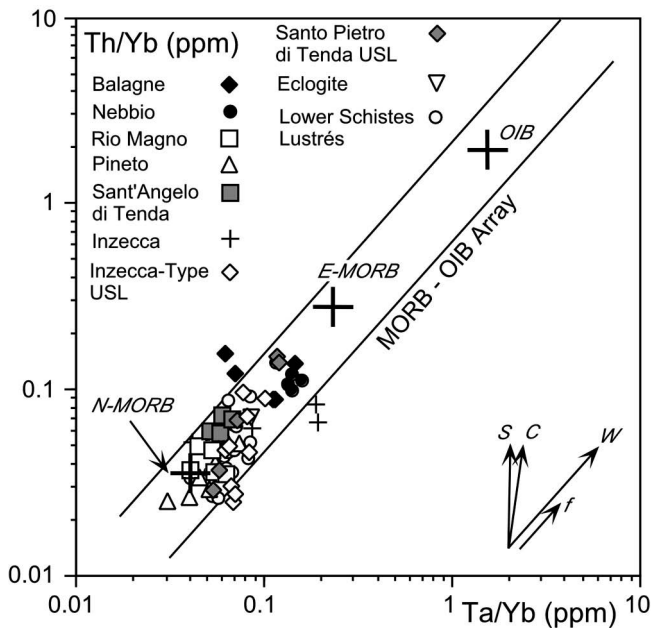
Fig. 4 - Th/Yb vs. Ta/Yb diagram for volcanic and metavolcanic rocks from Corsica ophiolites. Modified after Pearce (1982). The vectors of enrichment are: S = subduction zone; C = crustal contamination; W = within-plate; f = fractional crystallization. Compositions of typical N-MORB, E-MORB and OIB (large crosses) are from Sun and McDonough (1989).

The chondrite-normalized REE patterns for the metabasites from the different localities are very similar (Fig. 6b, d, f). They show marked LREE depletion with respect MREE, mild LREE/HREE depletion, and mild HREE fractionation with respect to MREE (Table 3). Apart from the generally low HREE contents, the HFSE and REE composition is compatible with that of N-MORB. In addition, all metabasites from the LSL unit have HFSE and REE compositions quite similar to those of N-MORB from the Internal Ligurides (Fig. 6a-d).

Eclogites of the Voplajola Unit

Eclogites studied in this paper are basaltic in composition (Table 2), with Mg# ranging from 51.9 - 58.2. Most likely, they represent moderately differentiated basalts. The most striking geochemical features are flat N-MORB normalized HFSE patterns. Compared to other metabasites from Corsica ophiolites, no Th, Ta depletion and P, Zr enrichment relative to the other HFSE can be observed (Fig. 6e). They only show Nb negative anomalies. The chondrite-normalized REE patterns show depletion in LREE with respect to MREE (Fig. 6f, Table 3). MREE and HREE show rather flat patterns, with $(Sm/Yb)_N$ ratios ranging from 0.89 - 1.07. The overall HFSE and REE composition resemble those observed in typical modern N-MORBs, as well as those of N-MORB from the Internal Ligurides (Fig. 6e, f).

PETROGENESIS

Magmatic evolution

Much of the compositional variation within the different ophiolitic units reflects the control by fractional crystallization. Most of the rocks studied in this paper have Mg# of less than 70 (Table 2), that is, lower than the Mg# > 70 inferred for primary melts of MORB-type plagioclase-bearing lherzolite (Sinton and Detrick, 1992). As seen in Fig. 2 relative to fractionation index, Zr, the broad increase in incompatible elements coupled with the rapid decrease in compatible Cr is characteristic of magmatic fractionation trends. In addition, the FeO_t increase with decreasing MgO abundance (not shown) requires that olivine segregation was not accompanied by loss of iron-rich phases, and the decreasing CaO/Al_2O_3 contents with increasing Zr content reflects control by plagioclase fractionation (Fig. 2). Accordingly, the occurrence of negative Eu anomalies among the REE (Figs. 3, 5, 6) implies that plagioclase fractionation was significant. Clinopyroxene segregation increases La/Sm and La/Yb in residual melts, but low pressure fractional crystallization of MORB involving olivine, plagioclase and clinopyroxene crystallization cannot cause large increases in La/Sm and La/Yb. This conclusion is valid for the Corsica basaltic and metabasaltic samples, which in general do not show any increase in La/Sm and La/Yb with increasing fractionation (Fig. 7). Only the most evolved basaltic andesites (Zr > 250 ppm) show a considerable La/Sm and La/Yb increase, suggesting that segregation of clinopyroxene was significant only in the relatively evolved rocks (Fig. 7). The restriction of clinopyroxene to ~ 30-40% of the segregating assemblage, observed through petrographic analyses, is also consistent with the small range in Sc content (Table 2). Projection of the basalt and metabasalt compositions from diopside onto the olivine-plagioclase-quartz plane (Fig. 8) supports the interpretation that most Corsica ophiolitic basaltic rocks evolved at pressures generally lower than 0.1 GPa within the oceanic crust by cotectic precipitation of olivine and plagioclase.

Mantle sources

Apart from the chemical variation ascribed to fractional crystallization processes, distinct normalized multi-element and REE patterns and ratios of incompatible elements, which are usually taken to reflect their source, suggest that basalts and metabasalts from the different ophiolitic units of Alpine Corsica may be derived from chemically distinct mantle sources. In particular, the wide variation of some incompatible element ratios (e.g., Zr/Y, from 1 to 10), and the fractionation among LREE, MREE, and HREE cannot be explained by fractional crystallization alone. For example, $(La/Yb)_N$ ratios (0.53-3.12) display greater variation than would be produced by low-pressure fractionation of common silicates. In addition, low-pressure fractional crystallization cannot explain the chondrite-normalized REE pattern crossing each other, as observed in the Balagne (Fig. 3b), Pineto (Fig. 3h), Inzecca-type (Fig. 5f, h), Santo Pietro di Tenda (Fig. 5j), and LSL (Fig. 6b, d) samples.

Alternatively, differential partial melting of lherzolite mantle (30% to 1% range) can accommodate much of the fractionation range shown by the REE. Nonetheless, the two main basalt and metabasite series, i.e. N-MORB and T-MORB, show significant differences in the HFSE and LREE patterns and degree of enrichment, as exhibited by N-MORB normalized distributions of Figs. 3, 5, 6.

Fig. 4 displays a mantle array for asthenospheric melts between a depleted N-MORB source and an enriched OIB-plume source. Except samples from the top of the Balagne volcanic sequence, the variation for both T- and N-MORBs from Corsica ophiolites and metaophiolites falls within the trend defined by the mantle array suggesting that a chemical
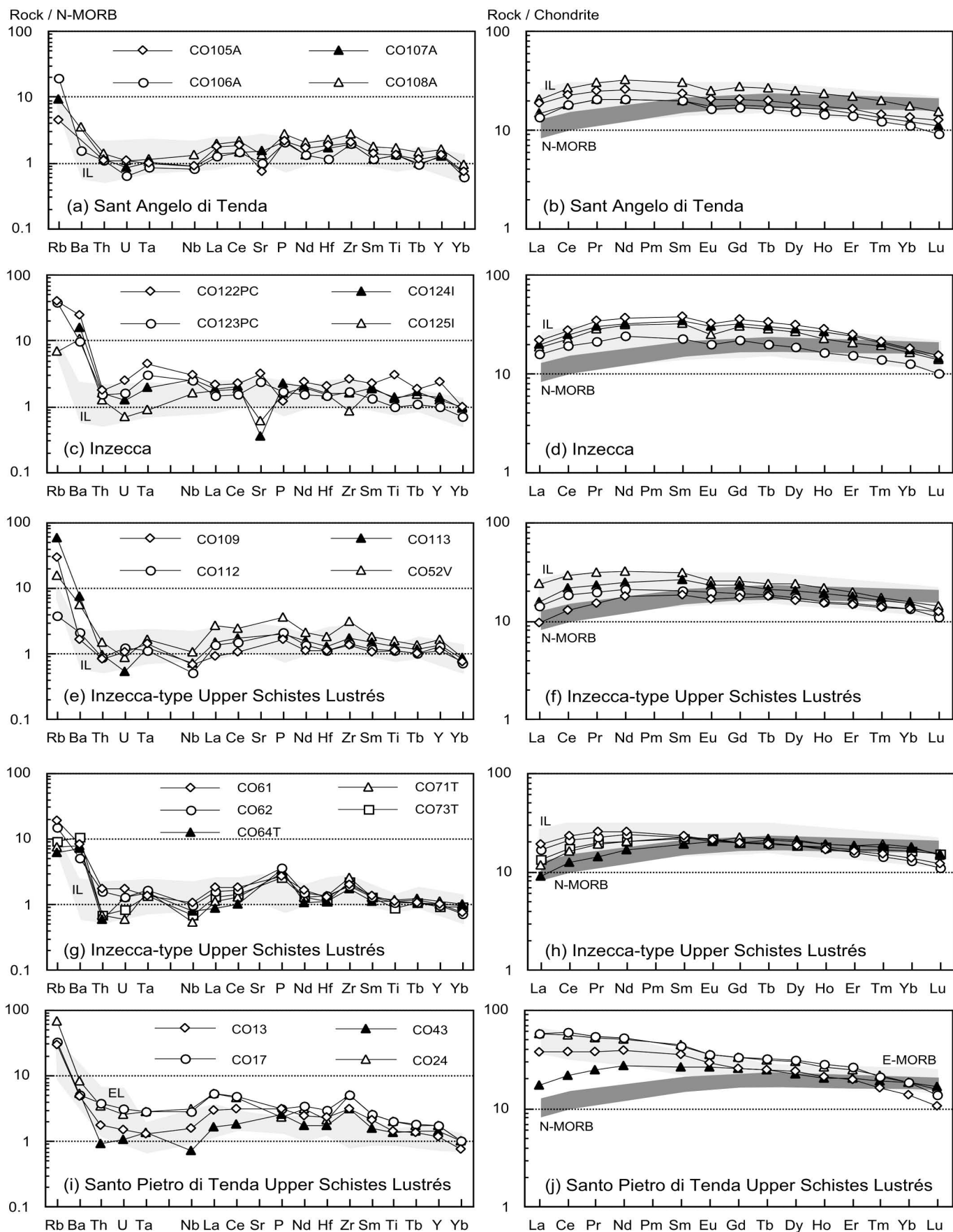
Fig. 5 - N-MORB normalized incompatible element and chondrite-normalized REE patterns for metavolcanic rocks from various units of the Upper Schistes Lustrés. Normalizing values are from Sun and McDonough (1989). Compositional variation (gray fields) of ophiolitic basalts from the External Ligurides (EL) of Northern Apennine (data from: Vannucci et al., 1993; Marroni et al., 1998; Montanini et al., 2008), ophiolitic basalts from the Internal Ligurides (IL) of Northern Apennine (data from: Venturelli et al., 1981; Ottonello et al., 1984; Cortesogno and Gaggero, 1992), as well as normal-type mid-ocean ridge basalts (N-MORB) and enriched-type mid-ocean ridge basalts (E-MORB) from modern oceanic settings (data from: Le Roex, 1987) are reported for comparison.
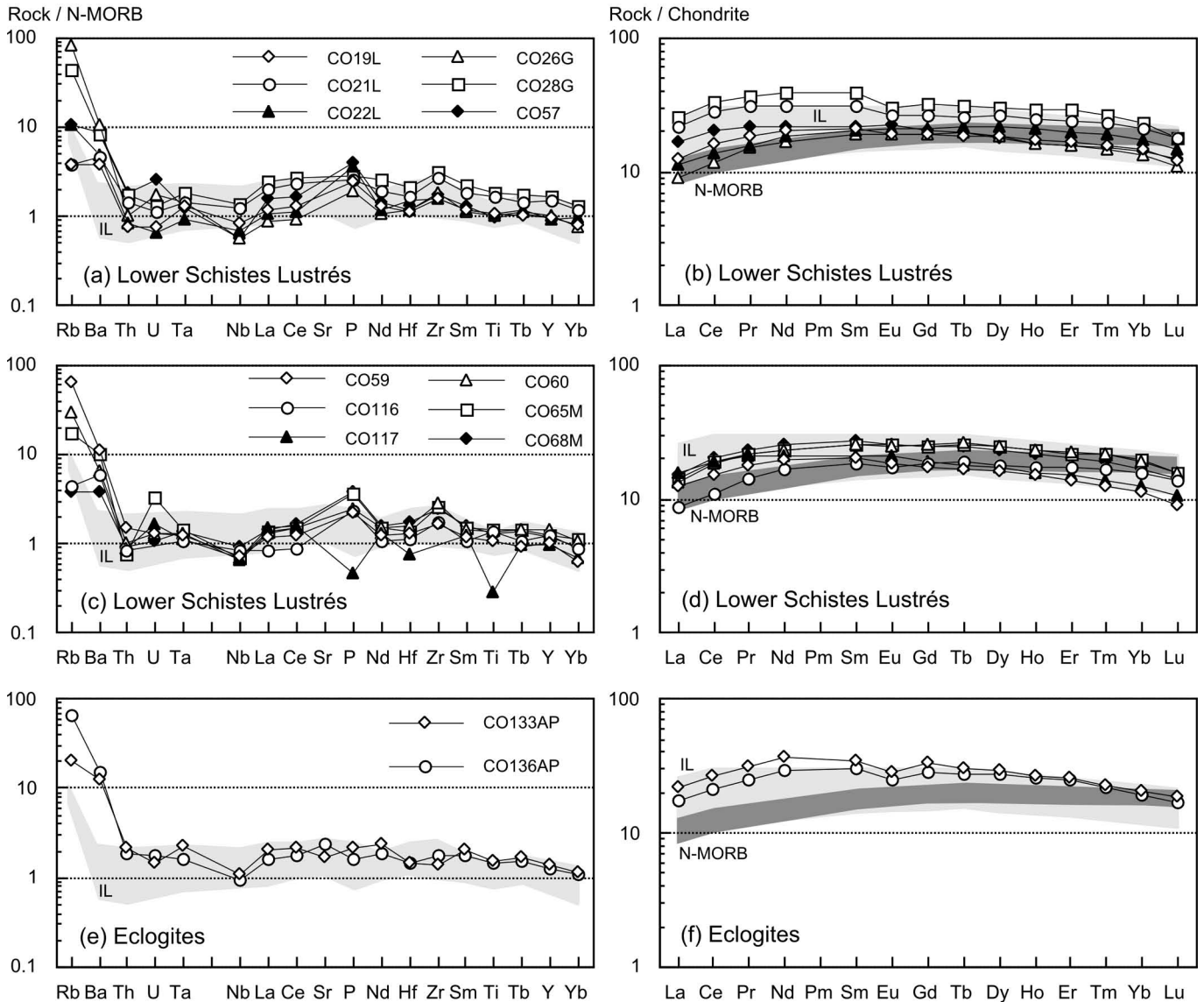
Fig. 6 - N-MORB normalized incompatible element and chondrite-normalized REE patterns for metavolcanic rocks from the Lower Schistes Lustrés (a, b) and Eclogite (c, d) Units. Normalizing values are from Sun and McDonough (1989). Compositional variation (gray fields) ophiolitic basalts from the Internal Ligurides (IL) of Northern Apennine (data from: Venturelli et al., 1981; Ottonello et al., 1984; Cortesogno and Gaggero, 1992) and normal-type mid-ocean ridge basalts (N-MORB) from modern oceanic settings (data from: Le Roex, 1987) are reported for comparison.

influence of a lower crust component was very limited or absent.

The variable degrees of enrichment exhibited by N-MORBs and T-MORBs can be considered a result from variable mixing between depleted and enriched asthenospheric sources or, alternatively, from different degree of partial melting. Ratios of highly incompatible trace elements, such as Ce/Y and La/Yb, are usually little influenced by small extents of fractional crystallization, and are expected to reflect either the source characteristics or the degree of partial melting (Saunders et al., 1988). Ce and La are more incompatible than Y and Yb, respectively; consequently, the rocks representing the smallest degree of partial melting or derived from more enriched sources exhibit the highest Ce/Y and $(La/Yb)_N$ ratios. From Fig. 9 it can be observed that basalts and metabasalts having T-MORB affinity display comparatively higher Ce/Y and $(La/Yb)_N$ ratios, which are comparable with those observed in modern primitive E-MORBs (Sun and McDonough, 1989), and possibly represent melts derived from enriched MORB type sub-oceanic mantle sources or by small degree of partial melting.

An estimation of the composition of primary magmas and relative mantle sources can be obtained using hygromagmatophile element ratios. These elements are weakly fractionated during partial melting and fractional crystallization and, therefore, in a diagram where ratio vs. ratio of hygromagmatophile elements are plotted, the population of samples originating from chemically different mantle sources will plot along distinct correlation lines representing the elemental ratios in the source (Allègre and Minster, 1978). The Th/Ta vs. Th/Tb ratios for the analyzed rocks are plotted in Fig. 10, where basically two distinct groups of samples can be recognized. The first group includes T-MORBs from the Nebbio and Santo Pietro di Tenda Units, as well as metabasaltic dykes from the Inzecca Unit and basalts from the bottom of the Balagne sequence. These rocks are characterized by (Th/Ta)/(Th/Tb) ratios ranging from 3.5 to 2.0. The second group includes N-MORBs

Fig. 7 - La/Sm vs. Zr (a) and La/Yb vs. Zr (b) diagrams for volcanic and metavolcanic rocks from Corsica ophiolites.

Fig. 8 - Pseudo-ternary diagram of normative plagioclase-olivine-silica (Pl-Ol-Qz) projected from diopside (Walker et al., 1979) for volcanic and metavolcanic rocks from Corsica ophiolites. Solid phase boundaries from experimental melts obtained from anhydrous conditions (Hirose and Kushiro, 1993) are also projected.

net-bearing mafic/ultramafic layers. The latter hypothesis has been recently suggested by Montanini et al. (2008) for the genesis of External Liguride basalts from Northern Apennine, which are interpreted as the product of partial melting of sub-continental mantle at the continent-ocean transition. In addition, Piccardo (2008) suggested that the garnet signature of these basalts was produced by garnet-pyroxenite relics left in the depleted mantle melting source after the delamination and sinking of portions of the deep garnet-pyroxenite-bearing lithospheric mantle. Piccardo (2008) proposed that (a) the Triassic rifting stage of the Piedmont-Ligurian ocean caused subsolidus exhumation of the sub-continental lithospheric mantle, by means of kilometre-scale shear zones (see also Montanini et al., 2006); (b) the late Triassic - Lower Jurassic drifting stage was characterized by the upwelling of the underlying asthenosphere associated with the inception of partial melting of the asthenosphere and melt percolation through the overlying lithospheric mantle; (c) the following spreading (oceanic) stage was characterized by the complete failure of the continental crust, exposure at the sea floor along the axial zone of the basin of oceanic peridotites, and extrusion of MORB magmas above mantle peridotites along the axis of the basin. According to this model, the ocean-continent transition zone is characterized by the occurrence of sub-continental lithospheric mantle of the Europe-Adria system, while the more internal oceanic setting of the ancient Piedmont-Ligurian basin was characterized by the occurrence of sub-continental mantle deeply modified by asthenospheric melts and oceanic mantle.

Therefore, in order to test the hypothesis that the two main basaltic suites of Corsica ophiolites may have derived from differently enriched mantle sources, and to explain the geochemical characteristics observed in most of the studied rocks, a non-modal, batch partial melting modelling of depleted MORB-type asthenospheric source and enriched lithospheric source is presented in Fig. 11. A rigorous quantification of the melting processes is not possible as the composition of the mantle source is difficult to constrain. However, a semi-quantitative modelling of the REE can place some effective constraints for explaining the REE composition of the rocks studied herein and particularly for

from the Rio Magno, Pineto, LSL, USL, and Eclogite Units, as well as samples from the top of the Balagne and Inzecca Units. These are characterized by (Th/Ta)/(Th/Tb) ratios ranging from 3.5 to 7.0, which are comparable with those of basalts from both Internal and External Ligurides. The comparison of Th/Ta versus Th/Tb ratios for N-and T-MORBs support the conclusion outlined above, that is, these two main basaltic suites derived from different mantle sources.

As a distinguishing feature, the Corsica ophiolitic basaltic and metabasaltic rocks are characterized by the significant HREE/MREE fractionation and very high $(Sm/Yb)_N$ ratios (Table 2). This feature is commonly interpreted as a garnet signature (Niu et al., 2002, and references therein), which can be related either to a deep initiation of melting in the garnet peridotite stability field, or to the melting of an heterogeneous mantle source characterized by gar-

Fig. 9 - Ce/Y vs. (La/Yb)$_N$ diagram for volcanic and metavolcanic rocks from Corsica ophiolites. Normalizing values are from Sun and McDonough (1989). Compositional variation (gray fields) of ophiolitic basalts from the External Ligurides (EL) of Northern Apennine (data from: Vannucci et al., 1993; Marroni et al., 1998; Montanini et al., 2008) and ophiolitic basalts from the Internal Ligurides (IL) of Northern Apennine (data from: Venturelli et al., 1981; Ottonello et al., 1984; Cortesogno and Gaggero, 1992), as well as compositions of typical N-MORB and E-MORB (large crosses) (data from Sun and McDonough, 1989) are reported for comparison. Dashed fields encircle Corsica basalts and metabasites with T-MORB and N-MORB composition.
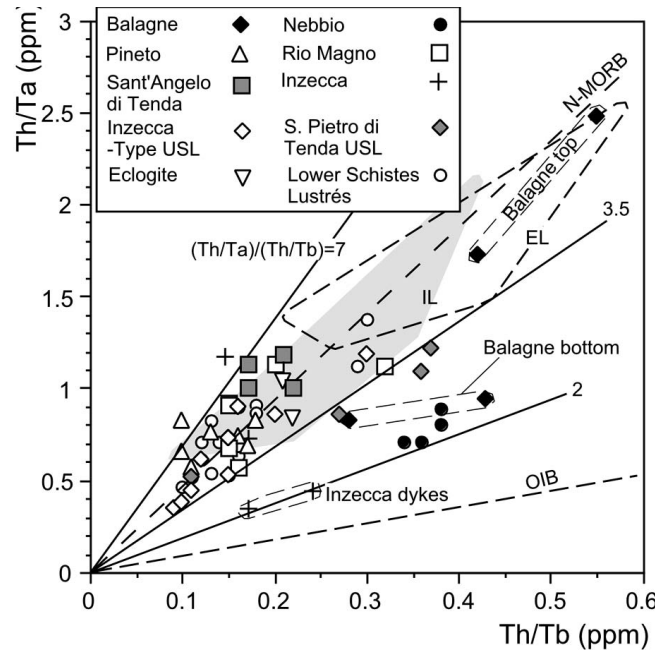
Fig. 10 - Th/Ta vs. Th/Tb diagram for volcanic and metavolcanic rocks from Corsica ophiolites. Compositional variation of ophiolitic basalts from the Internal Ligurides (IL) of Northern Apennine (data from: Venturelli et al., 1981; Ottonello et al., 1984; Cortesogno and Gaggero, 1992) and ophiolitic basalts from the External Ligurides (EL) of Northern Apennine (data from Montanini et al., 2008) are reported for comparison. Dashed lines represent (Th/Ta)/(Th/Tb) ratios for typical N-MORB and ocean-island basalt (OIB); data from Sun and McDonough (1989).

explaining the variable LREE/MREE ratios and the ubiquitous HREE/MREE fractionation.

The modal compositions and melting proportions of the different mantle sources assumed in the models of Fig. 11 are reported in Table 4, while the used REE distribution coefficient are from Kennedy et al. (1993) for olivine and orthopyroxene, from Kelemen et al. (1992) for spinel, and from Salters and Longhi (1996) for clinopyroxene and garnet. The model shown in Fig. 11a assumes a depleted MORB mantle (DMM) source (Workman and Hart, 2005) that starts to melt in the garnet lherzolite field and continues to larger degrees in the spinel lherzolite field. Various combinations of melting fraction in the garnet (from 0.5% to 2.0%, with 0.5% step) and spinel (from 2% to 15%, with variable steps) stability fields have been used in calculations; not all are shown in Fig. 11a. The most primitive N-MORB Corsica basalts and metabasalts have REE compositions, which are compatible with various calculated compositions ranging from 0.5% melting in the garnet stability field followed by 2.5% melting in the spinel field to 2% melting of garnet peridotite followed by 5% melting of spinel lherzolite (Fig. 11a). However, all the calculated compositions are characterized by (Sm/Yb)$_N$ and (Dy/Yb)$_N$ ratios generally lower than those observed in the studied samples, whereas the different combination of melting fractions in the garnet and spinel stability fields can explain the significant range of variation of (La/Sm)$_N$ ratios observed in the studied N-MORB rocks.

In Fig. 11b the partial melting model of DMM source

(Workman and Hart, 2005) characterized by garnet-pyroxenite layers (Montanini et al., 2008; Piccardo, 2008) is shown. This model assumes 20% melting of the garnet-pyroxenite source and mixing of these melts with melts generated from the partial melting of the depleted mantle source in the spinel-facies. It can be observed that the REE compositions of the most primitive N-MORB Corsica basalts and metabasalts are compatible with calculated compositions ranging from 2.5% to 8% melting of spinel peridotite characterized by garnet-pyroxenite layers (Fig. 11b). All the calculated compositions are have (Sm/Yb)$_N$ and (Dy/Yb)$_N$ ratios similar to those observed in the studied samples, whereas different degrees of melting can explain the range of variation of (La/Sm)$_N$ ratios observed in the studied N-MORB rocks.

Some basalts from the Rio Magno and Pineto Units do not show any significant garnet signature (Fig. 3f, h), having no HREE/MREE fractionation and comparatively lower (Sm/Yb)$_N$ and (Dy/Yb)$_N$ ratios. In Fig. 11c the partial melting model of DMM in the spinel-facies is shown. In fact, the REE composition of these basalts is compatible with low degree of partial melting (5%-8%) of a depleted (homogeneous) MORB mantle source in the spinel stability field.

Variable degrees of partial melting of a DMM source in the garnet and spinel facies, as well as of a DMM in the spinel-facies characterized by garnet-pyroxenite layers cannot generate the REE distribution observed in T-MORB rocks. Likewise, variable degrees of partial melting of ei-

ther a garnet or spinel lherzolite with a typical DMM composition cannot generate the (La/Yb)N and (Sm/Yb)N systematics of the Corsica T-MORB samples. In fact, melting a garnet lherzolite produces melts with much higher (La/Yb)N and (Sm/Yb)N ratios than the Corsica samples at reasonable degrees of melting (i.e., <10%), whereas melting a spinel lherzolite produces melts with lower (La/Yb)N and (Sm/Yb)N ratios than those observed in the Corsica samples (not shown). Therefore, according to the model proposed by Piccardo (2008), the most appropriate solution is to invoke a more enriched source than DMM, although no definite constraints about this source are available. Fig. 11d

illustrates melting curves for primitive lithospheric source (McDonough and Sun, 1995), assuming a small melt fraction formed under garnet-facies conditions and larger degrees of melting in the spinel stability field. The calculated melts do not match the REE compositions of the Corsica T-MORB. In particular, the calculated (La/Sm)N and (Sm/Yb)N ratios are, respectively, higher and lower than those observed in the studied rocks. By contrast, low degrees of partial melting (2.5%-5%) of a lithospheric source (McDonough and Sun, 1995) characterized by garnet-pyroxenite layers can explain the REE composition of Corsica T-MORBs (Fig. 11e).
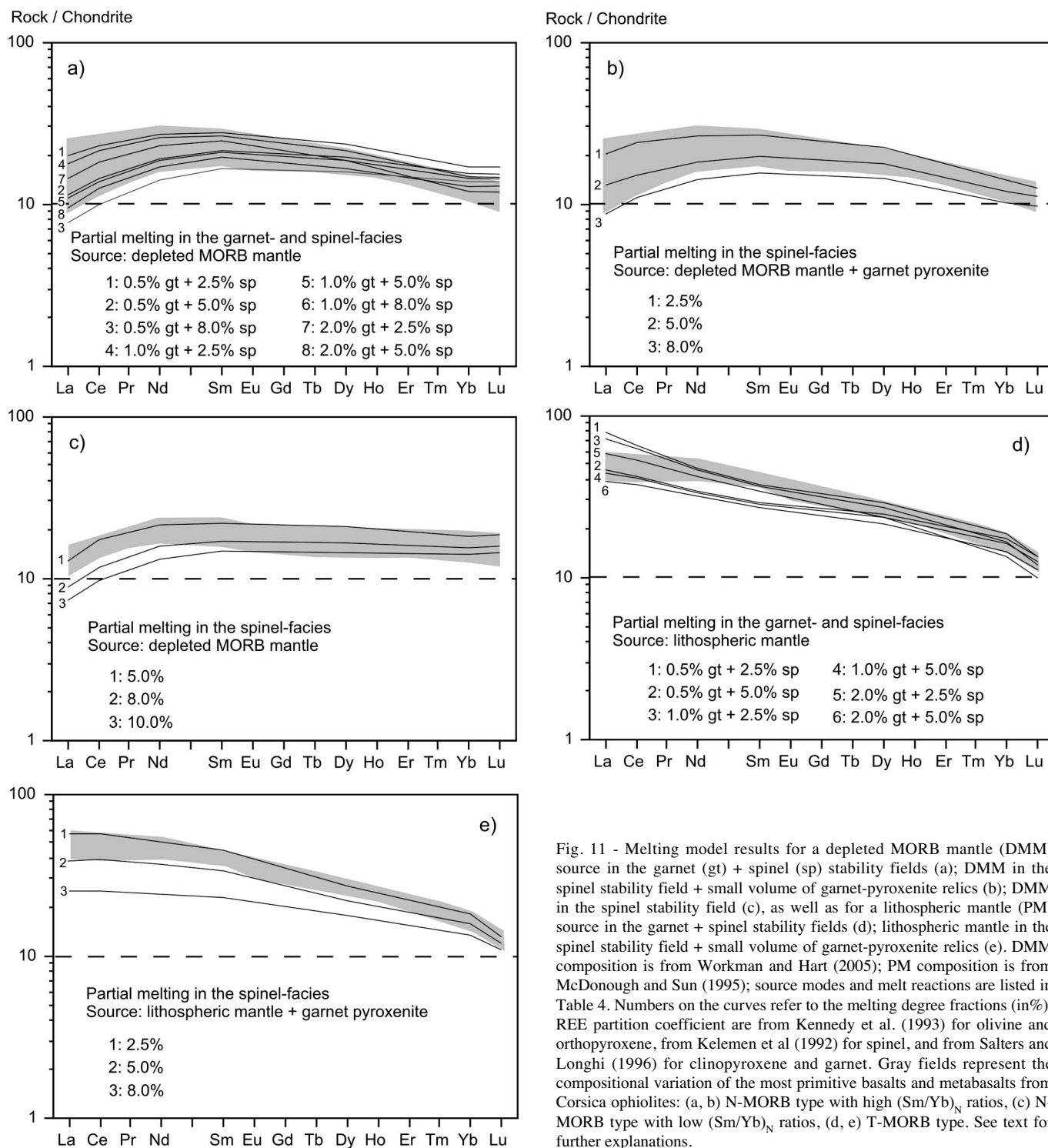
Fig. 11 - Melting model results for a depleted MORB mantle (DMM) source in the garnet (gt) + spinel (sp) stability fields (a); DMM in the spinel stability field + small volume of garnet-pyroxenite relics (b); DMM in the spinel stability field (c), as well as for a lithospheric mantle (PM) source in the garnet + spinel stability fields (d); lithospheric mantle in the spinel stability field + small volume of garnet-pyroxenite relics (e). DMM composition is from Workman and Hart (2005); PM composition is from McDonough and Sun (1995); source modes and melt reactions are listed in Table 4. Numbers on the curves refer to the melting degree fractions (in%). REE partition coefficient are from Kennedy et al. (1993) for olivine and orthopyroxene, from Kelemen et al (1992) for spinel, and from Salters and Longhi (1996) for clinopyroxene and garnet. Gray fields represent the compositional variation of the most primitive basalts and metabasalts from Corsica ophiolites: (a, b) N-MORB type with high (Sm/Yb)N ratios, (c) N-MORB type with low (Sm/Yb)N ratios, (d, e) T-MORB type. See text for further explanations.

Table 4 - Initial compositions and melting modes of the sources used in the melting models.

Source Composition	DMM (a)		PM (b)	Gt-Px.te (c)
	Garnet-facies	Spinel-facies	Spinel-facies	
Source Mode	(d)	(a)	(d)	(c)
Ol	0.57	0.57	0.53	
Opx	0.21	0.28	0.27	
Cpx	0.13	0.13	0.17	0.6
Gt	0.09			0.4
Sp		0.02	0.03	
Melting Mode	(d)	(d)	(d)	(c)
Ol	0.04	-0.06	0.04	
Opx	-0.19	0.28	-0.19	
Cpx	1.04	0.67	1.04	0.6
Gt	0.11			0.4
Sp		0.11	0.11	

Abbreviations, DMM: depleted MORB mantle; PM: Primitive mantle; Gt-Px.te: garnet-pyroxenite. Data source: (a) Workman and Hart (2005); (b) McDonough and Sun (1995); (c) Montanini et al. (2008); (d) Kinzler (1997).

CONCLUSIONS

Irrespective of the metamorphic evolution, two main compositional groups occur throughout Alpine Corsica: (a) a group with N-MORB characteristics (the volumetrically most abundant) with marked LREE/MREE depletion (La_N/Sm_N = 0.47-0.81), low Ce/Y and high Th/Ta ratios; (b) a group with T-MORB composition (volumetrically subordinate and restricted to the Santo Pietro di Tenda and Nebbio Units and to the bottom of the Balagne Unit) showing slight depletion or mild enrichment in LREE with respect to MREE (La_N/Sm_N = 0.90-1.32), high Ce/Y and low Th/Ta ratios. Low-pressure fractional crystallization has generally played a major role in controlling the compositional variations observed within each group of basaltic and metabasaltic rocks. However, the wide variation of some incompatible element ratios (e.g., Zr/Y, Ta/Yb, Th/Yb, Th/Tb, Th/Ta, Ce/Y) and the different fractionation among LREE, MREE, and HREE observed in N- and T-MORB from the different ophiolitic units of Alpine Corsica suggest that these two groups of rocks may have been derived from chemically distinct mantle sources. Moreover, most of the samples are variably depleted in HREE with respect to MREE contents (Sm_N/Yb_N = 1.23-2.57). Such a HREE fractionation is commonly interpreted as a garnet signature, which can be related to the melting of a heterogeneous mantle source characterized by garnet-bearing mafic/ultramafic layers (Montanini et al., 2008; Piccardo, 2008).

In light of the observations from the previous chapter, it is concluded that the N-MORBs from the Rio Magno, Pineto, Sant'Angelo di Tenda, LSL, USL and Eclogite Units, having quite similar hygromagmatophile element compositions, have derived from compositionally similar mantle sources and that much of the internal chemical variation in these rocks is more likely to be the consequence of different degrees of partial melting (from 2.5% to 8%) of similar mantle sources, each undergoing similar low-pressure fractionation, rather than a consequence of different enrichments of their mantle sources. According to the melting models illustrated in the previous chapter, this mantle source is most likely represented by a spinel-facies MORB-type depleted mantle containing garnet-pyroxenite relics of lithospheric origin. By contrast, T-MORBs have derived from primary melts originated from partial heterogeneous, garnet-pyroxenite bearing lithospheric mantle sources.

The variation in hygromagmatophile element (Fig. 10) and REE compositions (Fig. 3b) observed from the bottom to the top of the Balagne sequence suggest a change in mantle source from more enriched to less enriched compositions. On the other hand, dykes from the bottom of the Inzecca series are characterized by very different hygromagmatophile element composition with respect to metabasites from the top of the sequence (Fig. 10). However, no significant differences in REE ratios (Fig. 5d) or incompatible element composition (Fig. 9) between these two groups of rocks can be observed. It is therefore concluded that the Inzecca metabasites, though having different Th and Ta depletion, most likely derived from a similar MORB-type depleted mantle source.

According to the model proposed by Piccardo (2008) for the evolution of the Piedmont-Ligurian basin, the T-MORB sequences from the Balagne, Nebbio and Santo Pietro di Tenda Units may have originated in the ocean-continent transition zone. The present-day external position in the ophiolitic pile of these units (Fig. 1) and the continental-derived sedimentary covers of the Balagne and Nebbio Units (Principi et al., 2004, and references therein) further support this hypothesis. By contrast, the N-MORB sequences from all other ophiolitic units may have originated in a more internal paleo-oceanic position, as also inferred by the characteristics of their sedimentary covers. It can also be speculated that the Balagne sequence, showing geochemical variation from the bottom to the top of the sequence related to a change in mantle source from more enriched to less enriched compositions, may record the transition from lithospheric to asthenospheric mantle sources in the ocean-continent transition zone.

Finally, the systematic investigation of Corsica ophiolitic basaltic and metabasaltic rocks reveal some new aspects, which differ from what previously reported in literature. They may provide useful constraints for further studies on the entire pre-orogenic and syn-orogenic evolution of the Alpine Corsica orogenic belt. The most relevant are: (a) the N-MORB composition of part of the Balagne sequence and (b) the occurrence of T-MORB rocks within the USL Complex, which imply the involvement of the most external (transitional) oceanic crust within the deep subduction zone.

REFERENCES

Allègre C.J. and Minster J.F., 1978. Quantitative models of trace element behaviour in magmatic processes. Earth Planet. Sci. Lett., 38: 1-25.

Beccaluva L., Ohnenstetter D., Ohnenstetter M. and Venturelli G., 1977. The Trace Element geochemistry of Corsican Ophiolites. Contrib. Mineral. Petrol., 64: 11-31.

Beccaluva L., Ohnenstetter D. and Ohnenstetter M., 1979. Geochemical discrimination between ocean-floor and island-arc tholeiites-application to some ophiolites. Can. J. Earth Sci., 16: 1874-1882.

Bortolotti V. and Principi G., 2005. Tethyan ophiolites and Pangea break-up. The Island Arc, 14: 442-470.

Brunet C., Monié P., Jolivet L. and Cadet J.-P., 2000. Migration of compression and extension in the Tyrrhenian Sea from 40Ar/39Ar ages on micas along a transect from Corsica to Tuscany. Tectonophysics, 321: 127-155.

Caron J.M., Delcey R., Scius H., Essein J.P., Fraipont P., Mawhin B. and Reuber I., 1979. Répartition cartographique des principaux types des séries dans les Schistes Lustrés de Corse. C. R. Acad. Sci. Paris, 288: 1363-1366.

Cortesogno L. and Gaggero L., 1992. The basaltic dikes in the Bracco gabbroic massif: petrology of the earliest phases of basaltic activity in the northern Apennines ophiolites. Ofioliti, 17: 183 198.

De Wever P. and Danelian T., 1995. Supra-ophiolitic radiolarites from Alpine Corsica (France). Mém. Géol. Lausanne, 23: 731-735.

Durand-Delga M., 1978. Corse. Guides géologiques régionaux, Masson, Paris, 208 pp.

Durand-Delga M., 1984. Principaux traits de la Corse Alpine et corrélations avec les Alpes Ligures. Mem. Soc. Geol. It., 28: 285-329.

Durand-Delga M., Peybernès B. and Rossi P., 1997. Arguments en faveur de la position, au Jurassique, des ophiolites de Balagne (Haute-Corse, France) au voisinage de la marge continentale européenne. C. R. Acad. Sci. Paris, 32: 973-998.

Gardin S., Marino M., Monechi S. and Principi G., 1994. Biostratigraphy and sedimentology of Cretaceous Ligurid Flysch: paleogeography implication. Mem. Soc. Geol. It., 48: 219-235.

Gibbons W., Waters C. and Warburton J., 1986. The blueschist facies Schistes Lustrés of Alpine Corsica: a review. Geol. Soc. Am. Mem., 164: 301-311.

Hirose K. and Kushiro I., 1993. Partial melting of dry peridotites at high pressures: determination of compositions of melts segregated from peridotite using aggregates of diamond. Earth Planet. Sci. Lett., 114: 477-489.

Kelemen P.B., Dick H.J.B. and Quick J.E., 1992. Formation of harzburgite by pervasive melt/rock reaction in the upper mantle. Nature, 358: 635-641.

Kennedy A.K., Lofgren G.E. and Wasserburg G.J., 1993. An experimental study of trace element partitioning between olivine, orthopyroxene and melt in chondrules: equilibrium values and kinetic effects. Earth Planet. Sci. Lett., 115: 177-195.

Kinzler R.J., 1997. Melting of mantle peridotite at pressures approaching the spinel to garnet transition: application to mid-ocean ridge basalt petrogenesis. J. Geophys. Res., 102: 853-874.

Lachance G.R. and Trail R.J., 1966. Practical solution to the matrix problem in X-ray analysis. Can. Spectr., 11: 43-48.

Lahondère D., 1996. Les schistes bleus et les éclogites à lawsonite des unités continentales et océaniques de la Corse alpine. Doc. BRGM 240, 285 pp.

Lahondère D. and Guerrot C., 1997. Sm-Nd dating of Alpine eclogitic metamorphism in Corsica: evidence for Late Cretaceous subduction beneath the Corsican-Sardinian block. Géol. France, 3: 3-11.

Le Roex A.P., 1987. Source region of mid-ocean ridge basalts: evidence for enrichment processes. In: M.A. Menzies and C.J. Hawkesworth (Eds.), Mantle metasomatism, Academic Press, London, p. 389-419.

Malavieille J., Chemenda A. and Larroque C., 1998. Evolutionary model for Alpine Corsica: mechanism for ophiolite emplacement and exhumation of high-pressure rocks. Terra Nova, 10: 317-322.

Maluski H., 1977. Application de la méthode ^{40}Ar/^{39}Ar aux minéraux des roches cristallines perturbées par les événements thermiques et tectoniques en Corse. Bull. Soc. Géol. France, 194: 849-855.

Marino M., Monechi S. and Principi G., 1995. New calcareous nannofossil data on the Cretaceous-Eocene age of Corsica turbidites. Riv. It. Paleont. Strat., 101: 49-62.

Marroni M., Molli G., Montanini A. and Tribuzio R., 1998. The association of continental crust rocks with ophiolites in the Northern Apennines (Italy): implications for the continent-ocean transition in the Western Tethys. Tectonophysics, 292: 43-66.

Marroni M. and Pandolfi L., 2003. Deformation history of the ophiolite sequence from the Balagne Nappe, northern Corsica: insights in the tectonic evolution of the Alpine Corsica. Geol. J., 38: 67-83.

McDonough W.F. and Sun S.-S., 1995. The composition of the earth. Chem. Geol., 120: 223-253.

Montanini A., Tribuzio R. and Anczkiewicz R., 2006. Exhumation history of a garnet pyroxenite-bearing mantle section from a continent-ocean transition (Northern Apennine ophiolites, Italy). J. Petrol., 47: 1943-1971.

Montanini A., Tribuzio R. and Vernia L., 2008. Petrogenesis of basalts and gabbros from an ancient continent-ocean transition (External Liguride ophiolites, Northern Italy). Lithos, 101: 453-479.

Nardi R., Puccinelli A. and Verani M., 1978. Carta geologica della Balagne "sedimentaria" (Corsica) alla scala 1:25.000 e note illustrative. Boll. Soc. Geol. It., 97: 3-22.

Niu Y., Bideau D., Hekinian R. and Batiza R., 2002. Mantle compositional control on the extent of mantle melting, crust production, gravity anomaly, ridge morphology, and ridge segmentation: a case study at the Mid-Atlantic Ridge 33-35°N. Earth Planet. Sci. Lett., 186: 383-399.

Ohnenstetter D., Ohnenstetter M. and Rocci G., 1976. Étude des métamorphismes successifs des cumulats ophiolitiques de Corse. Bull. Soc. Géol. France, 18 (1): 115-134.

Ohnenstetter M., Ohnenstetter D., Vidal P., Cornichet J., Hermitte D. and Mace J., 1981. Crystallization and age of zircon from Corsican ophiolitic albitites: consequences for oceanic expansion in Jurassic time. Earth Planet. Sci. Lett., 54: 397-408.

Ottonello G., Joron J.L. and Piccardo G.B., 1984. Rare Earth and 3d transition element geochemistry of peridotitic rocks: II. Ligurian peridotites and associated basalts. J. Petrol., 25: 373-393.

Padoa E. and Durand-Delga M., 2001. L'unité ophiolitique du Rio Magno en Corse Alpine, élément des Ligurides de l'Apennin septentrional. C. R. Acad. Sci. Paris, Sci. Terre Planètes, 333: 285-293.

Padoa E., Saccani E. and Durand-Delga M., 2001. Structural and geochemical data on the Rio Magno Unit: evidences of a new "apenninic" ophiolitic unit in Alpine Corsica and its geodynamic implications, Terra Nova, 13: 135-142.

Padoa E., Saccani E. and Durand-Delga M., 2002. The Rio Magno Unit (Alpine Corsica): a review of its structural, stratigraphical and geochemical features and their geodynamic implications. Ofioliti, 27: 31-42.

Pearce J.A., 1982. Trace element characteristics of lavas from destructive plate boundaries. In: R.S. Thorpe (Ed.), Andesites. Wiley, New York, p. 525-548.

Pearce J.A., 1983. Role of the Sub-continental lithosphere in magma genesis at active continental margin. In: C.J. Hawkesworth and M.J. Norry (Eds.), Continental basalts and mantle xenoliths. Shiva, Nantwich, p. 230-249.

Pearce J.A. and Norry M.J., 1979. Petrogenetic implications of Ti, Zr, Y, and Nb variations in volcanic rocks. Contrib. Mineral. Petrol., 69: 33-47.

Piccardo G.B., 2008. The Jurassic Ligurian Tethys, a fossil ultra-slow-spreading ocean: the mantle perspective. In: M. Coltorti

and ecM. Grégoire (Eds.), Metasomatism in oceanic and continental mantle. Geol. Soc. London Sp. Publ., 293: 11-34.

Principi G. and Treves B., 1984. Il sistema Corso-Apenninico come prisma di accrezione. Riflessi sul problema generale del limite Alpi-Apennini. Mem. Soc. Geol. It., 28: 549-576.

Principi G., Bortolotti V., Chiari M., Cortesogno L., Gaggero L., Marcucci M., Saccani E. and Treves B., 2004. The Pre-orogenic volcano-sedimentary covers of the western Tethys oceanic basin: A review. Ofioliti, 29: 177-211.

Rossi P., Cocherie A., Lahondère D. and Fanning C.M., 2002. La marge européenne de la Téthys jurassique en Corse: datation de trondhjémites de Balagne et indices de croûte continentale sous le domaine Balano-Ligure: C. R. Acad. Sci. Paris, 334: 313-322.

Rossi P., Durand-Delga M., Caron J.M., Guieu G., Conchon O., Libourel G. and Loÿe-Pilot M.D., 1994. Carte Géologique de la France au 1:50.000 "Corte" et notice explicative de la feuille, BRGM nr. 1110, Orléans, France.

Saccani E., Padoa E. and Tassinari R., 2000. Preliminary data on the Pineto gabbroic Massif and Nebbio basalts: progress toward the geochemical characterization of Alpine Corsica ophiolites. Ofioliti, 25: 75-85.

Sagri M., Aiello E. and Certini L., 1982. Le unità torbiditiche cretacee della Corsica. Rend. Soc. Geol. It., 5: 87-91.

Salters V.J.M. and Longhi J., 1996. Partitioning of trace elements during primary melting of MORB mantle. Goldschmidt Meet., Hidelberg.

Saunders A.D., Norry M.J. and Tarney J., 1988. Origin of MORB and chemically-depleted mantle reservoirs: trace element constraints. In: M.A. Menzies and K.G. Cox (Eds.), Oceanic and continental lithosphere: similarities and differences. J. Petrol., Spec. Vol. 1988: 414-445.

Shervais J.W., 1982. Ti-V plots and the petrogenesis of modern ophiolitic lavas. Earth Planet. Sci. Lett., 59: 101-118.

Sinton J.M. and Detrick R.S., 1992. Mid-ocean ridge magma chambers. J. Geophys. Res., 97: 197-216.

Sun S.-S. and McDonough W.F., 1989. Chemical and isotopic systematics of ocean basalts: Implications for mantle composition and processes. In: A.D. Saunders and M.J. Norry (Eds.), Magmatism in the ocean basins. Geol. Soc. London Spec. Publ., 42: 313-346.

Vannucci R., Rampone E., Piccardo G.B., Ottolini L. and Bottazzi P., 1993. Ophiolitic magmatism in the Ligurian Tethys: An ion microprobe study of basaltic clinopyroxenes. Contrib. Mineral. Petrol., 115: 123-137.

Venturelli G., Capedri S., Thorpe R.S. and Potts P.J., 1979. Rare-earth and other trace element distribution in some ophiolitic metabasalts of Corsica. Chem. Geol., 24: 339-353.

Venturelli G., Thorpe R.S. and Potts P.J., 1981. Rare earth and trace element characteristics of ophiolitic metabasalts from the Alpine-Apennine belt. Earth Planet. Sci. Lett., 53: 109-123.

Walker D., Shibata T. and DeLong S.E., 1979. Abyssal tholeiite from the Ooceanographer Fracture Zone. II Phase equilibria and mixing. Contrib. Mineral. Petrol., 70: 111-125.

Warburton J., 1986. The ophiolite-bearing Schistes Lustrés Nappe in Alpine Corsica: A model for the emplacement of ophiolites that have suffered HP/LT metamorphism. Geol. Soc. Am. Mem., 164: 313-331.

Workman R.K. and Hart S.R., 2005. Major and trace element composition of the depleted MORB mantle (DMM). Earth Planet. Sci. Lett., 231, 53-72.